

Perturbative chiral violations for domain-wall QCD with improved gauge actions

Stefano Capitani*

*Institut für Physik, FB Theoretische Physik
Universität Graz, A-8010 Graz, Austria*

We investigate, in the framework of perturbation theory at finite N_s , the effectiveness of improved gauge actions in suppressing the chiral violations of domain-wall fermions. Our calculations show substantial reductions of the residual mass when it is compared at the same value of the gauge coupling, the largest suppression being obtained when the DBW2 action is used. Similar effects can also be observed for a power-divergent mixing coefficient which is chirally suppressed. No significant reduction instead can be seen in the case of the difference between the vector and axial-vector renormalization constants when improved gauge actions are used in place of the plaquette action. We also find that one-loop perturbation theory is not an adequate tool to carry out comparisons at the same energy scale (of about 2 GeV), and in fact in this case even an enhancement of the chiral violations is frequently obtained.

PACS numbers: 12.38.Gc, 11.30.Rd, 11.30.Qc, 11.10.Gh

I. INTRODUCTION

It has been known for some time that using in the gauge sector improved actions instead of the simpler plaquette action can significantly reduce the amount of chiral symmetry breaking in Monte Carlo simulations of domain-wall fermions [1, 2] (for the latest results obtained using this kind of actions see Refs. [3, 4, 5, 6, 7, 8, 9, 10], and references therein). This effect has been related to the fact that, for a determined value of the lattice spacing a , the corresponding values of $\beta' = 6(1 - 8c_1)/g_0^2$ (where c_1 is a parameter introduced in Section II which describes the various actions) are larger for improved gauge actions than for the plaquette action, and the gauge fields are correspondingly smoother.

Renormalization factors for domain-wall fermions with improved gauge actions have been calculated in one-loop perturbation theory using the asymptotic propagators at large N_s (where N_s denotes the number of points in the fifth dimension). The renormalization factors of the quark wave function, the quark mass, the bilinear quark operators and many three- and four-quark operators can be found in [11, 12] for many improved gauge actions, and the renormalization constant of the first moment of the unpolarized parton distribution has been calculated using the Iwasaki action in [6]. Here we present the first calculations made with the exact theory at finite N_s for this kind of gauge actions, and we consider some quantities which can describe chiral violations.

In this article we investigate whether perturbation theory can, at least qualitatively, reproduce the suppressions of the chiral violations which have been observed in numerical simulations when improved gauge actions are used. In a previous perturbative work [13] we have in-

vestigated the residual mass (together with the difference between the vector and axial-vector renormalization constants and with a chirally suppressed mixing coefficient for a deep-inelastic operator) using, for finite values of N_s , the plaquette gauge action. Here we repeat those calculations using Symanzik improved gauge actions like the Lüscher-Weisz action [14] and renormalization group improved gauge actions like the Iwasaki action [15] and the DBW2 action [16, 17]. By repeating the computations of the same above mentioned quantities with all these improved actions we can then make a direct comparison of the corresponding results and investigate the reduction of the chiral violations attained by each of these actions. As was the case for the plaquette, in carrying out these investigations one of our principal aims is also to calculate how these quantities behave for several choices of N_s and of the domain-wall height (or Dirac mass) M .

Apart from the new gluon propagators, the basic features of the calculations presented here remain the same as in [13], and in order not to render this paper too cumbersome we do not show here again many of the Tables and formulae that are independent of the gauge action used and that can be found in that paper. This applies in particular to the $1 - \lambda$ contributions (in a general covariant gauge described by λ) at one loop, and to the anomalous dimensions. For notations, the action and the basic fermion propagators we also refer to [13], which the reader is invited to consult for a fuller understanding of the calculations carried out in the present paper.

This article is organized as follows. In Sect. II we give the explicit expression of the gluon propagators for the class of improved gauge actions that we employ, and in Sect. III we then present the results for the residual mass at finite N_s , showing how its suppression is achieved by these actions when the coupling is kept constant. In Sect. IV we give the results for the difference between the vector and axial-vector renormalization constants and for the power-divergent mixing (due to the breaking of chiral symmetry) of an operator which describes polarized par-

*stefano.capitani@uni-graz.at

ton distributions. In this case we find that not always the use of improved gauge actions produces a significant reduction in the magnitude of the results at the same gauge coupling. Finally, in Sect. V we make some concluding remarks. An Appendix reports a few Tables concerning results for the plaquette action, so as to ease comparisons and make clearer the reductions of the chiral violations achieved by improved gauge actions compared with the plaquette action.

II. PERTURBATION THEORY

We use the standard formulation of domain-wall fermions of Shamir [18] where the quarks are massless,

$$S_q^{DW} = \sum_x \sum_{s=1}^{N_s} \left[\frac{1}{2} \sum_{\mu} \left(\bar{\psi}_s(x) (\gamma_{\mu} + 1) U_{\mu}(x) \psi_s(x + \hat{\mu}) \right. \right.$$

$$\left. \begin{aligned} & - \bar{\psi}_s(x) (\gamma_{\mu} - 1) U_{\mu}^{\dagger}(x - \hat{\mu}) \psi_s(x - \hat{\mu}) \\ & + \left(\bar{\psi}_s(x) P_+ \psi_{s+1}(x) + \bar{\psi}_s(x) P_- \psi_{s-1}(x) \right) \\ & \left. + (M - 1 - 4) \bar{\psi}_s(x) \psi_s(x) \right], \end{aligned} \quad (1)$$

and with improved gauge actions in place of the Wilson plaquette action in the gauge sector. For what concerns the Feynman rules, the fermionic part is then the same as in [13], including the expressions for the quark-gluon vertices. The gluon propagators instead are different, and in covariant gauge their expression in momentum space is [19]

$$G_{\mu\nu}(k) = \frac{1}{(\widehat{k}^2)^2} \left((1 - A_{\mu\nu}(k)) \widehat{k}_{\mu} \widehat{k}_{\nu} + \delta_{\mu\nu} \sum_{\sigma} \widehat{k}_{\sigma}^2 A_{\nu\sigma}(k) \right) - (1 - \lambda) \frac{\widehat{k}_{\mu} \widehat{k}_{\nu}}{(\widehat{k}^2)^2}, \quad (2)$$

where $\widehat{k}_{\mu} = 2 \sin k_{\mu}/2$, and $A_{\mu\nu}$ is symmetric in μ and ν and given by

$$A_{\mu\nu}(k) = \frac{1 - \delta_{\mu\nu}}{\Delta(k)} \left[(\widehat{k}^2)^2 - c_1 \widehat{k}^2 \left(2 \sum_{\rho} \widehat{k}_{\rho}^4 + \widehat{k}^2 \sum_{\rho \neq \mu, \nu} \widehat{k}_{\rho}^2 \right) + c_1^2 \left(\left(\sum_{\rho} \widehat{k}_{\rho}^4 \right)^2 + \widehat{k}^2 \sum_{\rho} \widehat{k}_{\rho}^4 \sum_{\tau \neq \mu, \nu} \widehat{k}_{\tau}^2 + (\widehat{k}^2)^2 \prod_{\rho \neq \mu, \nu} \widehat{k}_{\rho}^2 \right) \right], \quad (3)$$

with

$$\Delta(k) = \left(\widehat{k}^2 - c_1 \sum_{\rho} \widehat{k}_{\rho}^4 \right) \left[\widehat{k}^2 - c_1 \left((\widehat{k}^2)^2 + \sum_{\tau} \widehat{k}_{\tau}^4 \right) + \frac{1}{2} c_1^2 \left((\widehat{k}^2)^3 + 2 \sum_{\tau} \widehat{k}_{\tau}^6 - \widehat{k}^2 \sum_{\tau} \widehat{k}_{\tau}^4 \right) \right] - 4c_1^3 \sum_{\rho} \widehat{k}_{\rho}^4 \prod_{\tau \neq \rho} \widehat{k}_{\tau}^2. \quad (4)$$

The parameter c_1 describes the various actions: the choice $c_1 = -1/12$ corresponds to the Lüscher-Weisz action, $c_1 = -0.331$ corresponds to the Iwasaki action and $c_1 = -1.40686$ corresponds to the DBW2 action. Putting $c_1 = 0$ one recovers the expression of the Wilson plaquette propagator. For completeness, we mention that for $c_1 \neq 0$ the gluon vertices are also different from the ones of the plaquette action, and in particular the expressions of the 3- and 4-gluon vertices can be found in [19]. However, these new gluon vertices are only needed beyond one loop for the quantities investigated in this paper, and thus they will not interest us here.

The above expression for the gluon propagators clearly shows that, for a generic one-loop matrix element between quark states, the part proportional to $1 - \lambda$, that is the difference between its results for the Landau and Feynman gauges, is exactly equal to what one obtains using the plaquette action. For this reason we do not need to compute this part again and report here the results referring to it. These numbers can be found in the appropriate Tables of [13].

We find it useful to remind that in [13] it was also found that for many quantities the part proportional to $1 - \lambda$ presents a nontrivial dependence on N_s and M . Thus, also in the case of improved gauge actions the results for the residual mass and in general for the renormalization factors and mixing coefficients turn out not to be gauge invariant. Furthermore, the anomalous dimensions of operators at finite N_s are also the same as in the plaquette case, and they are thus different from their continuum values and again depend on N_s and M .

In our computations we have used the symbolic manipulation program FORM [20] to perform the algebraic calculations, integrating afterwards the corresponding expressions by means of Fortran codes, as explained in [13].

III. RESIDUAL MASS

Although the quark fields are originally massless in the Lagrangian that we employ, the truncation of domain-wall fermions at finite N_s generates already at tree level

a nonvanishing residual mass of the physical fields [13, 21, 22]:

$$a m_{res}^{(0)} = -w_0^{N_s} (1 - w_0^2) = -(1 - M)^{N_s} M(2 - M). \quad (5)$$

From now on we use the abbreviation $w_0 = 1 - M$, and we remind that the physical fields that we use are the standard ones and given by

$$q(x) = P_+ \psi_1(x) + P_- \psi_{N_s}(x) \quad (6)$$

$$\bar{q}(x) = \bar{\psi}_{N_s}(x) P_+ + \bar{\psi}_1(x) P_-. \quad (7)$$

Since we work with even N_s , $m_{res}^{(0)}$ is always a negative quantity. Its values for several choices of N_s and M are collected in Table XXV in the Appendix, where they have already been multiplied for $16\pi^2$, so as to make them more homogeneous with the numbers that we then report for the one-loop diagrams.

Radiative corrections provide additional contributions to m_{res} . At one loop the critical (or residual) mass is determined by the formula

$$a m_{res}^{(1)} = -w_0^{N_s} (1 - w_0^2) - \bar{g}^2 \Sigma_0, \quad (8)$$

where Σ_0 is the term proportional to $1/a$ in the self-energy of the quark,

$$\Sigma_q(p) = \frac{\bar{g}^2}{1 - w_0^2} \left[\frac{\Sigma_0}{a} + i\not{p} \left(c_{\Sigma_1}^{(N_s, M)} \log a^2 p^2 + \Sigma_1 \right) - (i\not{p} - w_0^{N_s} (1 - w_0^2)) \frac{2w_0}{1 - w_0^2} \Sigma_3 \right]. \quad (9)$$

Indeed, at this order one can write

$$\begin{aligned} \langle q(-p) \bar{q}(p) \rangle_{1 \text{ loop}} &= \frac{1 - w_0^2}{i\not{p} - w_0^{N_s} (1 - w_0^2) - (1 - w_0^2) \Sigma_q(p)} \\ &= \frac{1 - w_0^2}{i\not{p} Z_2^{-1} + m_{res}^{(1)}} Z_w, \end{aligned} \quad (10)$$

from which Eq. (8) follows. More details on these expressions concerning the one-loop self-energy can be found in [13]. Here we only remind that we call $\bar{g}^2 = (g_0^2/16\pi^2) C_F$ (with $C_F = 4/3$ for QCD) and that Z_2 is the quark wave function renormalization factor, while Z_w generates an additive renormalization to w_0 and hence to the domain-wall height M [23]. We can see that the mass correction term of Eq. (8) vanishes when the theory describes exact chiral fermions, but becomes nonzero when computations are done at any finite N_s . In this case Σ_0 generates a finite additive renormalization to the quark mass, which is a measure of chiral violations. We associate the perturbative critical mass m_{res} , which defines the chiral limit when no explicit mass term appears in the Lagrangian, with the residual mass which in Monte Carlo simulations is derived from the symmetry-breaking term in the axial Ward identities.

At one loop two diagrams enter in the calculation of the residual mass, the half-circle (or sunset) and the tadpole diagrams, which at order zero in p contribute to Σ_0 . The result of the tadpole diagram can be given in a simple form, and is equal to

$$T_d^{(0)} = T_l^{(0)} \frac{1 - w_0^2}{(1 - w_0^{2N_s})^2} \left(N_s (1 + w_0^{2(N_s+1)}) w_0^{N_s-1} - 2 w_0^{N_s+1} \frac{1 - w_0^{2N_s}}{1 - w_0^2} \right), \quad (11)$$

where $T_l^{(0)}$ is (up to a sign) the result of the tadpole of order zero for Wilson fermions:

$$T_l^{(0)} = 40.517749 - 8\pi^2 Z_0 (1 - \lambda) \quad (12)$$

for the Lüscher-Weisz action,

$$T_l^{(0)} = 29.927709 - 8\pi^2 Z_0 (1 - \lambda) \quad (13)$$

for the Iwasaki action and

$$T_l^{(0)} = 19.715871 - 8\pi^2 Z_0 (1 - \lambda) \quad (14)$$

for the DBW2 action, where $Z_0 = 0.154933390231\dots$ is a well-known integral [24]. It is useful to remind that for the plaquette action one had instead $T_l^{(0)} = 48.932201 - 8\pi^2 Z_0 (1 - \lambda)$. The domain-wall result assumes the simple form of Eq. (11) because the tadpole diagram is diagonal in the indices of the extra dimension, and since the loop integration involves only the

gluon propagator, which can be factorized out, for any given pair of N_s and M the tadpole results for all gauge actions are just proportional to $T_l^{(0)}$. We give here (in Table I) the explicit numbers only for the DBW2 action, which is presently the most used in numerical simulations of domain-wall QCD; for the Lüscher-Weisz and Iwasaki actions a simple multiplication then suffices.

The results for the half-circle diagram of Σ_0 are shown (in Feynman gauge) in Tables II, III and IV for the Lüscher-Weisz, Iwasaki and DBW2 action respectively. In addition to running the standard numerical integration in 6 dimensions, we have also redone the computation of this diagram by hand, including the calculation of the gamma algebra and the explicit exact evaluation of the sums over the fifth-dimensional indices. The resulting expressions are then four-dimensional. This provides a rather strong check of our calculations, and also saves 2 dimensions in the numerical integration.

TABLE I: Coefficient of \bar{g}^2 for the tadpole contribution to Σ_0 , Eq. (11), in Feynman gauge for the DBW2 gauge action. For the Iwasaki action all entries have to be multiplied by 1.51795, and for the Lüscher-Weisz action all entries have to be multiplied by 2.05508.

M	$N_s = 8$	$N_s = 12$	$N_s = 16$	$N_s = 20$	$N_s = 24$	$N_s = 28$	$N_s = 32$	$N_s = 48$	$N_s = \infty$
0.1	6.08558	6.84244	6.79166	6.17209	5.26321	4.28400	3.36856	1.04552	0
0.2	7.38915	5.23011	3.11540	1.68275	0.85663	0.41950	0.19994	0.00879	0
0.3	5.08323	2.00488	0.67208	0.20721	0.06076	0.01723	0.00477	0.00002	0
0.4	2.43021	0.49784	0.08825	0.01451	0.00228	0.00035	0.00005	0.00000	0
0.5	0.84720	0.08183	0.00692	0.00055	0.00004	0.00000	0.00000	0.00000	0
0.6	0.20674	0.00807	0.00028	0.00001	0.00000	0.00000	0.00000	0.00000	0
0.7	0.03061	0.00038	0.00000	0.00000	0.00000	0.00000	0.00000	0.00000	0
0.8	0.00192	0.00000	0.00000	0.00000	0.00000	0.00000	0.00000	0.00000	0
0.9	0.00002	0.00000	0.00000	0.00000	0.00000	0.00000	0.00000	0.00000	0
1.0	0.00000	0.00000	0.00000	0.00000	0.00000	0.00000	0.00000	0.00000	0
1.1	-0.00002	0.00000	0.00000	0.00000	0.00000	0.00000	0.00000	0.00000	0
1.2	-0.00192	0.00000	0.00000	0.00000	0.00000	0.00000	0.00000	0.00000	0
1.3	-0.03061	-0.00038	0.00000	0.00000	0.00000	0.00000	0.00000	0.00000	0
1.4	-0.20674	-0.00807	-0.00028	-0.00001	0.00000	0.00000	0.00000	0.00000	0
1.5	-0.84720	-0.08183	-0.00692	-0.00055	-0.00004	0.00000	0.00000	0.00000	0
1.6	-2.43021	-0.49784	-0.08825	-0.01451	-0.00228	-0.00035	-0.00005	0.00000	0
1.7	-5.08323	-2.00488	-0.67208	-0.20721	-0.06076	-0.01723	-0.00477	-0.00002	0
1.8	-7.38915	-5.23011	-3.11540	-1.68275	-0.85663	-0.41950	-0.19994	-0.00879	0
1.9	-6.08558	-6.84244	-6.79166	-6.17209	-5.26321	-4.28400	-3.36856	-1.04552	0

TABLE II: Coefficient of \bar{g}^2 for the contribution of the half-circle diagram to Σ_0 , in Feynman gauge for the Lüscher-Weisz gauge action.

M	$N_s = 8$	$N_s = 12$	$N_s = 16$	$N_s = 20$	$N_s = 24$	$N_s = 28$	$N_s = 32$	$N_s = 48$	$N_s = \infty$
0.1	1.85305	1.69896	1.41789	1.12004	0.85404	0.63588	0.46559	0.12125	0
0.2	2.33907	1.42243	0.76566	0.38732	0.18868	0.08958	0.04173	0.00173	0
0.3	1.83151	0.67820	0.21995	0.06655	0.01928	0.00542	0.00147	0.00001	0
0.4	1.08252	0.22556	0.04045	0.00670	0.00104	0.00015	0.00002	0.00000	0
0.5	0.50879	0.05403	0.00482	0.00038	0.00003	0.00000	0.00000	0.00000	0
0.6	0.19223	0.00935	0.00036	0.00001	0.00000	0.00000	0.00000	0.00000	0
0.7	0.05966	0.00129	0.00002	0.00000	0.00000	0.00000	0.00000	0.00000	0
0.8	0.01726	0.00025	0.00000	0.00000	0.00000	0.00000	0.00000	0.00000	0
0.9	0.00635	0.00010	0.00000	0.00000	0.00000	0.00000	0.00000	0.00000	0
1.0	0.00339	0.00007	0.00000	0.00000	0.00000	0.00000	0.00000	0.00000	0
1.1	0.00229	0.00005	0.00000	0.00000	0.00000	0.00000	0.00000	0.00000	0
1.2	0.00268	0.00005	0.00000	0.00000	0.00000	0.00000	0.00000	0.00000	0
1.3	0.01527	0.00021	0.00000	0.00000	0.00000	0.00000	0.00000	0.00000	0
1.4	0.08659	0.00335	0.00011	0.00000	0.00000	0.00000	0.00000	0.00000	0
1.5	0.32093	0.03003	0.00249	0.00018	0.00001	0.00000	0.00000	0.00000	0
1.6	0.84348	0.16170	0.02776	0.00448	0.00067	0.00010	0.00001	0.00000	0
1.7	1.65276	0.57478	0.18073	0.05366	0.01535	0.00427	0.00115	0.00000	0
1.8	2.37106	1.36227	0.71569	0.35718	0.17245	0.08134	0.03770	0.00154	0
1.9	2.08894	1.80335	1.46797	1.14614	0.86894	0.64513	0.47169	0.12268	0

We can express Σ_0 , the residual mass and the other quantities presented in this paper in the form

$$A + (1 - \lambda) B, \quad (15)$$

where A and $A + B$ provide the answers in Feynman and Landau gauge respectively, and B is a number which remains the same when using fermion formulations rather diverse like domain-wall with an infinite extent of the fifth dimension, Wilson or overlap. Since, as we have noticed in the previous Section, B remains also the same whether

the plaquette action or an improved gluon action is used, we refer for its results to the corresponding Tables in [13].

The values of Σ_0 which come out after our results for the tadpole and half-circle diagrams are added together are reported in Tables V, VI and VII. The values of $am_{res}^{(1)}$ which one obtains after the contribution of the tree-level residual mass is finally included are shown in Tables VIII to XIII for the three improved gauge actions considered. In the case of the DBW2 action, given that is

TABLE III: Coefficient of \bar{g}^2 for the contribution of the half-circle diagram to Σ_0 , in Feynman gauge for the Iwasaki gauge action.

M	$N_s = 8$	$N_s = 12$	$N_s = 16$	$N_s = 20$	$N_s = 24$	$N_s = 28$	$N_s = 32$	$N_s = 48$	$N_s = \infty$
0.1	0.50821	0.21779	-0.03162	-0.18502	-0.25188	-0.26034	-0.23689	-0.09532	0
0.2	0.63587	0.22998	0.06006	0.00769	-0.00410	-0.00467	-0.00314	-0.00024	0
0.3	0.57859	0.18254	0.05361	0.01524	0.00423	0.00115	0.00029	0.00000	0
0.4	0.41985	0.08688	0.01562	0.00259	0.00039	0.00005	0.00001	0.00000	0
0.5	0.23861	0.02652	0.00242	0.00019	0.00001	0.00000	0.00000	0.00000	0
0.6	0.10593	0.00549	0.00022	0.00001	0.00000	0.00000	0.00000	0.00000	0
0.7	0.03747	0.00086	0.00002	0.00000	0.00000	0.00000	0.00000	0.00000	0
0.8	0.01169	0.00017	0.00000	0.00000	0.00000	0.00000	0.00000	0.00000	0
0.9	0.00428	0.00007	0.00000	0.00000	0.00000	0.00000	0.00000	0.00000	0
1.0	0.00222	0.00004	0.00000	0.00000	0.00000	0.00000	0.00000	0.00000	0
1.1	0.00146	0.00003	0.00000	0.00000	0.00000	0.00000	0.00000	0.00000	0
1.2	0.00218	0.00003	0.00000	0.00000	0.00000	0.00000	0.00000	0.00000	0
1.3	0.01789	0.00023	0.00000	0.00000	0.00000	0.00000	0.00000	0.00000	0
1.4	0.11072	0.00428	0.00014	0.00000	0.00000	0.00000	0.00000	0.00000	0
1.5	0.43174	0.04077	0.00340	0.00025	0.00002	0.00000	0.00000	0.00000	0
1.6	1.18690	0.23278	0.04042	0.00656	0.00100	0.00015	0.00002	0.00000	0
1.7	2.41466	0.88093	0.28421	0.08571	0.02477	0.00695	0.00189	0.00001	0
1.8	3.52723	2.20554	1.22505	0.63440	0.31424	0.15100	0.07098	0.00301	0
1.9	3.06494	2.94845	2.63010	2.21616	1.78901	1.39824	1.06623	0.30874	0

 TABLE IV: Coefficient of \bar{g}^2 for the contribution of the half-circle diagram to Σ_0 , in Feynman gauge for the DBW2 gauge action.

M	$N_s = 8$	$N_s = 12$	$N_s = 16$	$N_s = 20$	$N_s = 24$	$N_s = 28$	$N_s = 32$	$N_s = 48$	$N_s = \infty$
0.1	-1.10030	-1.53568	-1.73593	-1.71261	-1.54242	-1.30396	-1.05364	-0.34630	0
0.2	-1.38867	-1.17537	-0.76769	-0.43649	-0.22928	-0.11464	-0.05545	-0.00253	0
0.3	-0.90559	-0.40170	-0.14203	-0.04505	-0.01344	-0.00386	-0.00110	-0.00001	0
0.4	-0.36485	-0.07724	-0.01379	-0.00227	-0.00038	-0.00006	-0.00001	0.00000	0
0.5	-0.08232	-0.00635	-0.00045	-0.00004	0.00000	0.00000	0.00000	0.00000	0
0.6	0.00264	0.00080	0.00004	0.00000	0.00000	0.00000	0.00000	0.00000	0
0.7	0.01059	0.00032	0.00001	0.00000	0.00000	0.00000	0.00000	0.00000	0
0.8	0.00494	0.00007	0.00000	0.00000	0.00000	0.00000	0.00000	0.00000	0
0.9	0.00188	0.00003	0.00000	0.00000	0.00000	0.00000	0.00000	0.00000	0
1.0	0.00092	0.00002	0.00000	0.00000	0.00000	0.00000	0.00000	0.00000	0
1.1	0.00059	0.00001	0.00000	0.00000	0.00000	0.00000	0.00000	0.00000	0
1.2	0.00169	0.00001	0.00000	0.00000	0.00000	0.00000	0.00000	0.00000	0
1.3	0.02083	0.00025	0.00000	0.00000	0.00000	0.00000	0.00000	0.00000	0
1.4	0.13739	0.00532	0.00017	0.00001	0.00000	0.00000	0.00000	0.00000	0
1.5	0.55390	0.05271	0.00442	0.00033	0.00002	0.00000	0.00000	0.00000	0
1.6	1.56471	0.31178	0.05455	0.00890	0.00137	0.00020	0.00003	0.00000	0
1.7	3.24961	1.22111	0.39990	0.12166	0.03537	0.00997	0.00273	0.00001	0
1.8	4.78426	3.14023	1.79449	0.94576	0.47393	0.22960	0.10857	0.00468	0
1.9	4.11043	4.20697	3.92344	3.41545	2.82481	2.24857	1.73889	0.52014	0

the most used in numerical simulations, we explicitly give the results for two choices of the bare coupling, $\beta = 6.0$ and $\beta = 5.2$, and in both Feynman and Landau gauges. This also helps to illustrate the fact that for the DBW2 action the violations of gauge invariance are here rather pronounced. The Lüscher-Weisz and Iwasaki actions behave in this respect in a similar way, the main difference being that the residual mass is less small and the relative violations of gauge invariance are less large. For these two actions we only show here the Tables corresponding to $\beta = 5.2$ in Landau gauge. Other choices of β as well

as results in Feynman gauge can be easily derived from the primary results provided for Σ_0 .

In the plaquette case we had observed [13] that when the one-loop corrections are taken into account, the residual mass, which is negative at tree level, changes sign and becomes positive. This also happens for the Lüscher-Weisz and Iwasaki actions, and (except for very small N_s , or M very close to 2) for the DBW2 action. We can check from the various Tables here provided that also for the improved gauge actions the residual mass $am_{res}^{(1)}$ happens to have the same sign of the critical mass of Wilson

TABLE V: Coefficient of \bar{g}^2 for the complete result of Σ_0 , in Feynman gauge for the Lüscher-Weisz gauge action.

M	$N_s = 8$	$N_s = 12$	$N_s = 16$	$N_s = 20$	$N_s = 24$	$N_s = 28$	$N_s = 32$	$N_s = 48$	$N_s = \infty$
0.1	14.35942	15.76075	15.37532	13.80421	11.67038	9.43986	7.38826	5.42456	0
0.2	17.52439	12.17074	7.16806	3.84552	1.94912	0.95169	0.45262	0.19370	0
0.3	12.27798	4.79840	1.60113	0.49238	0.14415	0.04083	0.01128	0.00267	0
0.4	6.07680	1.24867	0.22182	0.03653	0.00572	0.00087	0.00013	0.00002	0
0.5	2.24985	0.22220	0.01904	0.00150	0.00011	0.00001	0.00000	0.00000	0
0.6	0.61709	0.02594	0.00093	0.00003	0.00000	0.00000	0.00000	0.00000	0
0.7	0.12258	0.00206	0.00003	0.00000	0.00000	0.00000	0.00000	0.00000	0
0.8	0.02120	0.00025	0.00000	0.00000	0.00000	0.00000	0.00000	0.00000	0
0.9	0.00638	0.00010	0.00000	0.00000	0.00000	0.00000	0.00000	0.00000	0
1.0	0.00339	0.00007	0.00000	0.00000	0.00000	0.00000	0.00000	0.00000	0
1.1	0.00226	0.00005	0.00000	0.00000	0.00000	0.00000	0.00000	0.00000	0
1.2	-0.00126	0.00005	0.00000	0.00000	0.00000	0.00000	0.00000	0.00000	0
1.3	-0.04765	-0.00056	0.00000	0.00000	0.00000	0.00000	0.00000	0.00000	0
1.4	-0.33827	-0.01324	-0.00046	-0.00001	0.00000	0.00000	0.00000	0.00000	0
1.5	-1.42013	-0.13814	-0.01173	-0.00094	-0.00007	-0.00001	0.00000	0.00000	0
1.6	-4.15080	-0.86142	-0.15360	-0.02535	-0.00401	-0.00062	-0.00009	-0.00002	0
1.7	-8.79371	-3.54541	-1.20046	-0.37218	-0.10952	-0.03114	-0.00866	-0.00266	0
1.8	-12.81426	-9.38605	-5.68671	-3.10102	-1.58799	-0.78077	-0.37320	-0.19043	0
1.9	-10.41742	-12.25844	-12.48946	-11.53802	-9.94739	-8.15885	-6.45097	-5.18063	0

TABLE VI: Coefficient of \bar{g}^2 for the complete result of Σ_0 , in Feynman gauge for the Iwasaki gauge action.

M	$N_s = 8$	$N_s = 12$	$N_s = 16$	$N_s = 20$	$N_s = 24$	$N_s = 28$	$N_s = 32$	$N_s = 48$	$N_s = \infty$
0.1	9.74581	10.60427	10.27779	9.18391	7.73742	6.24256	4.87641	3.82187	0
0.2	11.85223	8.16903	4.78908	2.56202	1.29622	0.63211	0.30036	0.14156	0
0.3	8.29469	3.22585	1.07380	0.32977	0.09646	0.02731	0.00753	0.00197	0
0.4	4.10879	0.84259	0.14958	0.02462	0.00385	0.00058	0.00009	0.00001	0
0.5	1.52461	0.15073	0.01293	0.00102	0.00008	0.00001	0.00000	0.00000	0
0.6	0.41974	0.01774	0.00064	0.00002	0.00000	0.00000	0.00000	0.00000	0
0.7	0.08394	0.00143	0.00002	0.00000	0.00000	0.00000	0.00000	0.00000	0
0.8	0.01460	0.00017	0.00000	0.00000	0.00000	0.00000	0.00000	0.00000	0
0.9	0.00431	0.00007	0.00000	0.00000	0.00000	0.00000	0.00000	0.00000	0
1.0	0.00222	0.00004	0.00000	0.00000	0.00000	0.00000	0.00000	0.00000	0
1.1	0.00144	0.00003	0.00000	0.00000	0.00000	0.00000	0.00000	0.00000	0
1.2	-0.00073	0.00003	0.00000	0.00000	0.00000	0.00000	0.00000	0.00000	0
1.3	-0.02859	-0.00034	0.00000	0.00000	0.00000	0.00000	0.00000	0.00000	0
1.4	-0.20310	-0.00797	-0.00028	-0.00001	0.00000	0.00000	0.00000	0.00000	0
1.5	-0.85426	-0.08344	-0.00710	-0.00057	-0.00004	0.00000	0.00000	0.00000	0
1.6	-2.50204	-0.52292	-0.09354	-0.01547	-0.00246	-0.00038	-0.00006	-0.00001	0
1.7	-5.30143	-2.16238	-0.73598	-0.22883	-0.06746	-0.01920	-0.00535	-0.00196	0
1.8	-7.68914	-5.73352	-3.50397	-1.91993	-0.98607	-0.48578	-0.23252	-0.13878	0
1.9	-6.17267	-7.43803	-7.67930	-7.15278	-6.20028	-5.10466	-4.04708	-3.60846	0

fermions (i.e., is positive) only for $M \gtrsim 1.2$, exactly as in the case of the plaquette action. This is the region of M we are interested in. The value $M \simeq 1.2$ arises as a consequence of the additive renormalization undergone by w_0 (in this case, at one loop), and this shows that improved gauge actions do not behave too differently in this respect.

If we compare the results derived in this paper with the residual mass that was obtained using the plaquette gauge action [13], we can see that the use of improved gauge actions produces, for the same choice of g_0 , a significant suppression of $am_{res}^{(1)}$. A consistent picture of

this effect can be gathered by looking at the numbers for $\beta = 5.2$ in the Landau gauge for the various actions, contained in Tables XXVII, VIII, IX and XIII. We can immediately see that the Iwasaki action gives a stronger suppression than the Lüscher-Weisz action. Although not properly consistent at this order in g_0 , we can also have a look at what happens in the case $N_s = 16$ and $M = 1.8$, which are typical values chosen in the numerical simulations. For these two actions, and for this choice, one-loop perturbative calculations give a residual mass which is respectively about two-thirds and one-third of the plaquette value. A very interesting outcome is that

TABLE VII: Coefficient of \bar{g}^2 for the complete result of Σ_0 , in Feynman gauge for the DBW2 gauge action.

M	$N_s = 8$	$N_s = 12$	$N_s = 16$	$N_s = 20$	$N_s = 24$	$N_s = 28$	$N_s = 32$	$N_s = 48$	$N_s = \infty$
0.1	4.98528	5.30676	5.05573	4.45949	3.72080	2.98004	2.31491	2.23429	0
0.2	6.00048	4.05474	2.34771	1.24626	0.62735	0.30486	0.14449	0.09088	0
0.3	4.17765	1.60318	0.53006	0.16216	0.04732	0.01337	0.00368	0.00129	0
0.4	2.06536	0.42060	0.07446	0.01224	0.00190	0.00028	0.00004	0.00001	0
0.5	0.76488	0.07548	0.00647	0.00050	0.00004	0.00000	0.00000	0.00000	0
0.6	0.20938	0.00887	0.00032	0.00001	0.00000	0.00000	0.00000	0.00000	0
0.7	0.04121	0.00070	0.00001	0.00000	0.00000	0.00000	0.00000	0.00000	0
0.8	0.00686	0.00008	0.00000	0.00000	0.00000	0.00000	0.00000	0.00000	0
0.9	0.00189	0.00003	0.00000	0.00000	0.00000	0.00000	0.00000	0.00000	0
1.0	0.00092	0.00002	0.00000	0.00000	0.00000	0.00000	0.00000	0.00000	0
1.1	0.00057	0.00001	0.00000	0.00000	0.00000	0.00000	0.00000	0.00000	0
1.2	-0.00023	0.00001	0.00000	0.00000	0.00000	0.00000	0.00000	0.00000	0
1.3	-0.00978	-0.00012	0.00000	0.00000	0.00000	0.00000	0.00000	0.00000	0
1.4	-0.06935	-0.00275	-0.00010	0.00000	0.00000	0.00000	0.00000	0.00000	0
1.5	-0.29330	-0.02912	-0.00250	-0.00021	-0.00002	0.00000	0.00000	0.00000	0
1.6	-0.86550	-0.18607	-0.03370	-0.00561	-0.00091	-0.00014	-0.00002	-0.00001	0
1.7	-1.83363	-0.78377	-0.27219	-0.08555	-0.02539	-0.00726	-0.00204	-0.00129	0
1.8	-2.60489	-2.08988	-1.32091	-0.73700	-0.38269	-0.18990	-0.09137	-0.08873	0
1.9	-1.97515	-2.63547	-2.86822	-2.75664	-2.43840	-2.03543	-1.62967	-2.06044	0

TABLE VIII: Residual mass in lattice units at $\beta = 5.2$, in Landau gauge for the Lüscher-Weisz gauge action.

M	$N_s = 8$	$N_s = 12$	$N_s = 16$	$N_s = 20$	$N_s = 24$	$N_s = 28$	$N_s = 32$	$N_s = 48$	$N_s = \infty$
0.1	-0.21605	-0.20260	-0.18145	-0.15496	-0.12696	-0.10057	-0.07757	-0.04763	0
0.2	-0.22551	-0.14044	-0.07859	-0.04098	-0.02040	-0.00984	-0.00464	-0.00149	0
0.3	-0.14568	-0.05280	-0.01700	-0.00512	-0.00148	-0.00042	-0.00011	-0.00002	0
0.4	-0.06850	-0.01331	-0.00230	-0.00037	-0.00006	-0.00001	0.00000	0.00000	0
0.5	-0.02438	-0.00231	-0.00019	-0.00002	0.00000	0.00000	0.00000	0.00000	0
0.6	-0.00646	-0.00026	-0.00001	0.00000	0.00000	0.00000	0.00000	0.00000	0
0.7	-0.00124	-0.00002	0.00000	0.00000	0.00000	0.00000	0.00000	0.00000	0
0.8	-0.00021	0.00000	0.00000	0.00000	0.00000	0.00000	0.00000	0.00000	0
0.9	-0.00006	0.00000	0.00000	0.00000	0.00000	0.00000	0.00000	0.00000	0
1.0	-0.00003	0.00000	0.00000	0.00000	0.00000	0.00000	0.00000	0.00000	0
1.1	-0.00002	0.00000	0.00000	0.00000	0.00000	0.00000	0.00000	0.00000	0
1.2	0.00001	0.00000	0.00000	0.00000	0.00000	0.00000	0.00000	0.00000	0
1.3	0.00042	0.00001	0.00000	0.00000	0.00000	0.00000	0.00000	0.00000	0
1.4	0.00285	0.00012	0.00000	0.00000	0.00000	0.00000	0.00000	0.00000	0
1.5	0.01138	0.00120	0.00011	0.00001	0.00000	0.00000	0.00000	0.00000	0
1.6	0.03114	0.00724	0.00135	0.00023	0.00004	0.00001	0.00000	0.00000	0
1.7	0.05963	0.02849	0.01029	0.00330	0.00099	0.00029	0.00008	0.00002	0
1.8	0.07020	0.06959	0.04664	0.02670	0.01406	0.00704	0.00341	0.00123	0
1.9	0.02569	0.07052	0.09008	0.09195	0.08365	0.07088	0.05726	0.03713	0

the DBW2 action is the most effective in generating a large suppression. We can observe a general monotonic decrease of the residual mass when c_1 grows, however we can gather from Tables X to XIII that for the DBW2 action this suppression can at times go too far and for some choices of N_s and M we actually obtain (small) negative values for the residual mass.

We should note at this point that the dramatic suppression of the residual mass in the case of the DBW2 action is caused not only by the decreasing of the absolute value of the results for the tadpole (which are negative for $M > 1$), but also by the increasing of the results for

the half-circle diagram (which are positive). The numbers provided for $N_s = 16$ and $M = 1.8$ in Table XVII can summarize this behavior. We remind that Σ_0 , which is the sum of these two diagrams, enters with a negative sign in the one-loop formula for m_{res} , Eq. (8). At the end, what happens is that the total contribution of the one-loop diagrams becomes smaller as c_1 grows, and since the (negative) tree-level residual mass remains always the same for all gauge actions, for the DBW2 action the compensations between the tree-level and one-loop diagrams are much larger. The final numbers for $m_{res}^{(1)}$ are then decisively smaller for this action, and sometimes they even

TABLE IX: Residual mass in lattice units at $\beta = 5.2$, in Landau gauge for the Iwasaki gauge action.

M	$N_s = 8$	$N_s = 12$	$N_s = 16$	$N_s = 20$	$N_s = 24$	$N_s = 28$	$N_s = 32$	$N_s = 48$	$N_s = \infty$
0.1	-0.17110	-0.15236	-0.13179	-0.10995	-0.08865	-0.06942	-0.05309	-0.03202	0
0.2	-0.17025	-0.10145	-0.05542	-0.02847	-0.01404	-0.00672	-0.00315	-0.00098	0
0.3	-0.10687	-0.03748	-0.01187	-0.00354	-0.00102	-0.00028	-0.00008	-0.00001	0
0.4	-0.04933	-0.00936	-0.00160	-0.00026	-0.00004	-0.00001	0.00000	0.00000	0
0.5	-0.01731	-0.00161	-0.00013	-0.00001	0.00000	0.00000	0.00000	0.00000	0
0.6	-0.00453	-0.00018	-0.00001	0.00000	0.00000	0.00000	0.00000	0.00000	0
0.7	-0.00086	-0.00001	0.00000	0.00000	0.00000	0.00000	0.00000	0.00000	0
0.8	-0.00014	0.00000	0.00000	0.00000	0.00000	0.00000	0.00000	0.00000	0
0.9	-0.00004	0.00000	0.00000	0.00000	0.00000	0.00000	0.00000	0.00000	0
1.0	-0.00002	0.00000	0.00000	0.00000	0.00000	0.00000	0.00000	0.00000	0
1.1	-0.00001	0.00000	0.00000	0.00000	0.00000	0.00000	0.00000	0.00000	0
1.2	0.00001	0.00000	0.00000	0.00000	0.00000	0.00000	0.00000	0.00000	0
1.3	0.00023	0.00000	0.00000	0.00000	0.00000	0.00000	0.00000	0.00000	0
1.4	0.00153	0.00007	0.00000	0.00000	0.00000	0.00000	0.00000	0.00000	0
1.5	0.00586	0.00067	0.00006	0.00001	0.00000	0.00000	0.00000	0.00000	0
1.6	0.01508	0.00394	0.00077	0.00013	0.00002	0.00000	0.00000	0.00000	0
1.7	0.02561	0.01502	0.00577	0.00190	0.00058	0.00017	0.00005	0.00001	0
1.8	0.02027	0.03401	0.02538	0.01519	0.00820	0.00417	0.00204	0.00073	0
1.9	-0.01566	0.02356	0.04321	0.04923	0.04715	0.04113	0.03384	0.02181	0

TABLE X: Residual mass in lattice units at $\beta = 6$, in Feynman gauge for the DBW2 gauge action.

M	$N_s = 8$	$N_s = 12$	$N_s = 16$	$N_s = 20$	$N_s = 24$	$N_s = 28$	$N_s = 32$	$N_s = 48$	$N_s = \infty$
0.1	-0.12388	-0.09847	-0.07790	-0.06075	-0.04657	-0.03511	-0.02607	-0.02315	0
0.2	-0.11106	-0.05897	-0.02996	-0.01467	-0.00700	-0.00327	-0.00151	-0.00088	0
0.3	-0.06467	-0.02060	-0.00617	-0.00178	-0.00050	-0.00014	-0.00004	-0.00001	0
0.4	-0.02819	-0.00494	-0.00081	-0.00013	-0.00002	0.00000	0.00000	0.00000	0
0.5	-0.00939	-0.00082	-0.00007	0.00000	0.00000	0.00000	0.00000	0.00000	0
0.6	-0.00232	-0.00009	0.00000	0.00000	0.00000	0.00000	0.00000	0.00000	0
0.7	-0.00041	-0.00001	0.00000	0.00000	0.00000	0.00000	0.00000	0.00000	0
0.8	-0.00006	0.00000	0.00000	0.00000	0.00000	0.00000	0.00000	0.00000	0
0.9	-0.00002	0.00000	0.00000	0.00000	0.00000	0.00000	0.00000	0.00000	0
1.0	-0.00001	0.00000	0.00000	0.00000	0.00000	0.00000	0.00000	0.00000	0
1.1	0.00000	0.00000	0.00000	0.00000	0.00000	0.00000	0.00000	0.00000	0
1.2	0.00000	0.00000	0.00000	0.00000	0.00000	0.00000	0.00000	0.00000	0
1.3	0.00002	0.00000	0.00000	0.00000	0.00000	0.00000	0.00000	0.00000	0
1.4	0.00004	0.00001	0.00000	0.00000	0.00000	0.00000	0.00000	0.00000	0
1.5	-0.00045	0.00006	0.00001	0.00000	0.00000	0.00000	0.00000	0.00000	0
1.6	-0.00344	0.00018	0.00010	0.00002	0.00000	0.00000	0.00000	0.00000	0
1.7	-0.01392	-0.00044	0.00060	0.00032	0.00012	0.00004	0.00001	0.00001	0
1.8	-0.03840	-0.00709	0.00102	0.00207	0.00153	0.00091	0.00049	0.00063	0
1.9	-0.06511	-0.03141	-0.01099	0.00018	0.00543	0.00724	0.00724	0.01312	0

overshoot and become negative.

Thus far we have only discussed comparisons made at the same value of the coupling among the various actions, and we have provided numbers for situations in which g_0^2 is equal to 1 or near it. However, if we want to compare the results of the various actions at the same energy scale, we have to insert the appropriate values of g_0 belonging to each improved action for a given lattice spacing. The picture that comes out from such comparisons is then somewhat different. Let us take as an illustration the case of quenched QCD at 2 GeV, a scale that Monte Carlo simulations teach us to be reached for $\beta = 5.7$ when the Lüscher-Weisz action is used, for $\beta = 2.6$ when the

Iwasaki action is used, and for $\beta = 1.04$ when the DBW2 action is used. Note that here we maintain the definition of $\beta = 6/g_0^2$ also for the improved gauge actions, instead of $\beta' = 6(1 - 8c_1)/g_0^2$. The corresponding results for $am_{res}^{(1)}$ are collected in Tables XIV, XV and XVI. It is curious to notice from these Tables that the numbers obtained using the Iwasaki action are rather close to those obtained using the DBW2 action, and surprisingly they lie in general slightly above the plaquette values (which we report in Table XXVIII in the Appendix).

We have however to stress at this point that for the quenched DBW2 case at 2 GeV the gauge coupling as-

TABLE XI: Residual mass in lattice units at $\beta = 6$, in Landau gauge for the DBW2 gauge action.

M	$N_s = 8$	$N_s = 12$	$N_s = 16$	$N_s = 20$	$N_s = 24$	$N_s = 28$	$N_s = 32$	$N_s = 48$	$N_s = \infty$
0.1	-0.11900	-0.09447	-0.07482	-0.05848	-0.04493	-0.03395	-0.02526	-0.01492	0
0.2	-0.10619	-0.05648	-0.02877	-0.01412	-0.00675	-0.00316	-0.00145	-0.00044	0
0.3	-0.06178	-0.01972	-0.00592	-0.00171	-0.00048	-0.00013	-0.00004	-0.00001	0
0.4	-0.02693	-0.00473	-0.00078	-0.00012	-0.00002	0.00000	0.00000	0.00000	0
0.5	-0.00898	-0.00079	-0.00006	0.00000	0.00000	0.00000	0.00000	0.00000	0
0.6	-0.00223	-0.00009	0.00000	0.00000	0.00000	0.00000	0.00000	0.00000	0
0.7	-0.00040	-0.00001	0.00000	0.00000	0.00000	0.00000	0.00000	0.00000	0
0.8	-0.00006	0.00000	0.00000	0.00000	0.00000	0.00000	0.00000	0.00000	0
0.9	-0.00002	0.00000	0.00000	0.00000	0.00000	0.00000	0.00000	0.00000	0
1.0	-0.00001	0.00000	0.00000	0.00000	0.00000	0.00000	0.00000	0.00000	0
1.1	0.00000	0.00000	0.00000	0.00000	0.00000	0.00000	0.00000	0.00000	0
1.2	0.00000	0.00000	0.00000	0.00000	0.00000	0.00000	0.00000	0.00000	0
1.3	0.00004	0.00000	0.00000	0.00000	0.00000	0.00000	0.00000	0.00000	0
1.4	0.00013	0.00001	0.00000	0.00000	0.00000	0.00000	0.00000	0.00000	0
1.5	-0.00005	0.00010	0.00001	0.00000	0.00000	0.00000	0.00000	0.00000	0
1.6	-0.00219	0.00039	0.00014	0.00003	0.00001	0.00000	0.00000	0.00000	0
1.7	-0.01101	0.00043	0.00085	0.00039	0.00014	0.00004	0.00001	0.00000	0
1.8	-0.03342	-0.00459	0.00221	0.00262	0.00178	0.00102	0.00054	0.00019	0
1.9	-0.05992	-0.02729	-0.00787	0.00247	0.00708	0.00840	0.00805	0.00526	0

TABLE XII: Residual mass in lattice units at $\beta = 5.2$, in Feynman gauge for the DBW2 gauge action.

M	$N_s = 8$	$N_s = 12$	$N_s = 16$	$N_s = 20$	$N_s = 24$	$N_s = 28$	$N_s = 32$	$N_s = 48$	$N_s = \infty$
0.1	-0.13036	-0.10536	-0.08446	-0.06655	-0.05141	-0.03898	-0.02908	-0.02605	0
0.2	-0.11886	-0.06424	-0.03301	-0.01629	-0.00781	-0.00367	-0.00169	-0.00100	0
0.3	-0.07010	-0.02268	-0.00686	-0.00199	-0.00056	-0.00015	-0.00004	-0.00001	0
0.4	-0.03087	-0.00549	-0.00091	-0.00014	-0.00002	0.00000	0.00000	0.00000	0
0.5	-0.01038	-0.00092	-0.00007	-0.00001	0.00000	0.00000	0.00000	0.00000	0
0.6	-0.00259	-0.00010	0.00000	0.00000	0.00000	0.00000	0.00000	0.00000	0
0.7	-0.00046	-0.00001	0.00000	0.00000	0.00000	0.00000	0.00000	0.00000	0
0.8	-0.00007	0.00000	0.00000	0.00000	0.00000	0.00000	0.00000	0.00000	0
0.9	-0.00002	0.00000	0.00000	0.00000	0.00000	0.00000	0.00000	0.00000	0
1.0	-0.00001	0.00000	0.00000	0.00000	0.00000	0.00000	0.00000	0.00000	0
1.1	-0.00001	0.00000	0.00000	0.00000	0.00000	0.00000	0.00000	0.00000	0
1.2	0.00000	0.00000	0.00000	0.00000	0.00000	0.00000	0.00000	0.00000	0
1.3	0.00004	0.00000	0.00000	0.00000	0.00000	0.00000	0.00000	0.00000	0
1.4	0.00013	0.00001	0.00000	0.00000	0.00000	0.00000	0.00000	0.00000	0
1.5	-0.00007	0.00010	0.00001	0.00000	0.00000	0.00000	0.00000	0.00000	0
1.6	-0.00232	0.00042	0.00015	0.00003	0.00001	0.00000	0.00000	0.00000	0
1.7	-0.01154	0.00058	0.00096	0.00043	0.00015	0.00005	0.00001	0.00001	0
1.8	-0.03502	-0.00438	0.00274	0.00303	0.00203	0.00115	0.00060	0.00075	0
1.9	-0.06255	-0.02799	-0.00726	0.00376	0.00860	0.00989	0.00935	0.01579	0

sumes the value $g_0^2 = 5.77$, which appears to be somewhat too large to constitute a reasonable perturbative expansion coefficient. Moreover, such values of the coupling are derived solely from numerical simulations, and they then contain informations of nonperturbative nature as well, so that a mismatch can arise when one only takes into account the results of the one-loop diagrams calculated at these values of the coupling, that is when c_1 is not small.

Notice that the Lüscher-Weisz action gives in the above case the best results in terms of suppression, and indeed g_0^2 is still not too far from 1 for this action even at the scale of 2 GeV.

Although it is clear that one-loop perturbation theory encounters here some of its limitations and cannot provide the whole story, the small numbers for the residual mass that we can see in the Tables for the DBW2 action when g_0^2 is near 1 may qualitatively confirm the knowledge about the effects of improved gauge actions which has been gathered from numerical simulations in the past years. Since one-loop perturbation theory is in this case not fully adequate, 2-loop (and higher) corrections should be considered (at least for the Iwasaki and DBW2 actions) if one is interested in getting more reliable numbers. It looks like the two-loop contributions become indeed more and more important as c_1 grows,

TABLE XIII: Residual mass in lattice units at $\beta = 5.2$, in Landau gauge for the DBW2 gauge action.

M	$N_s = 8$	$N_s = 12$	$N_s = 16$	$N_s = 20$	$N_s = 24$	$N_s = 28$	$N_s = 32$	$N_s = 48$	$N_s = \infty$
0.1	-0.12472	-0.10075	-0.08091	-0.06392	-0.04952	-0.03764	-0.02814	-0.01655	0
0.2	-0.11324	-0.06137	-0.03163	-0.01566	-0.00752	-0.00354	-0.00163	-0.00049	0
0.3	-0.06676	-0.02167	-0.00657	-0.00191	-0.00054	-0.00015	-0.00004	-0.00001	0
0.4	-0.02942	-0.00525	-0.00087	-0.00014	-0.00002	0.00000	0.00000	0.00000	0
0.5	-0.00991	-0.00088	-0.00007	-0.00001	0.00000	0.00000	0.00000	0.00000	0
0.6	-0.00248	-0.00010	0.00000	0.00000	0.00000	0.00000	0.00000	0.00000	0
0.7	-0.00045	-0.00001	0.00000	0.00000	0.00000	0.00000	0.00000	0.00000	0
0.8	-0.00007	0.00000	0.00000	0.00000	0.00000	0.00000	0.00000	0.00000	0
0.9	-0.00002	0.00000	0.00000	0.00000	0.00000	0.00000	0.00000	0.00000	0
1.0	-0.00001	0.00000	0.00000	0.00000	0.00000	0.00000	0.00000	0.00000	0
1.1	-0.00001	0.00000	0.00000	0.00000	0.00000	0.00000	0.00000	0.00000	0
1.2	0.00000	0.00000	0.00000	0.00000	0.00000	0.00000	0.00000	0.00000	0
1.3	0.00005	0.00000	0.00000	0.00000	0.00000	0.00000	0.00000	0.00000	0
1.4	0.00023	0.00002	0.00000	0.00000	0.00000	0.00000	0.00000	0.00000	0
1.5	0.00040	0.00014	0.00002	0.00000	0.00000	0.00000	0.00000	0.00000	0
1.6	-0.00087	0.00066	0.00019	0.00004	0.00001	0.00000	0.00000	0.00000	0
1.7	-0.00818	0.00159	0.00125	0.00051	0.00017	0.00005	0.00002	0.00000	0
1.8	-0.02927	-0.00149	0.00411	0.00367	0.00232	0.00128	0.00066	0.00024	0
1.9	-0.05656	-0.02323	-0.00366	0.00640	0.01050	0.01123	0.01029	0.00673	0

TABLE XIV: Residual mass in lattice units at $\beta = 5.7$, in Landau gauge for the Lüscher-Weisz gauge action.

M	$N_s = 8$	$N_s = 12$	$N_s = 16$	$N_s = 20$	$N_s = 24$	$N_s = 28$	$N_s = 32$	$N_s = 48$	$N_s = \infty$
0.1	-0.20427	-0.18953	-0.16862	-0.14340	-0.11716	-0.09262	-0.07133	-0.04383	0
0.2	-0.21102	-0.13029	-0.07259	-0.03775	-0.01876	-0.00904	-0.00425	-0.00137	0
0.3	-0.13548	-0.04879	-0.01566	-0.00471	-0.00136	-0.00038	-0.00010	-0.00002	0
0.4	-0.06344	-0.01227	-0.00212	-0.00034	-0.00005	-0.00001	0.00000	0.00000	0
0.5	-0.02250	-0.00212	-0.00018	-0.00001	0.00000	0.00000	0.00000	0.00000	0
0.6	-0.00594	-0.00024	-0.00001	0.00000	0.00000	0.00000	0.00000	0.00000	0
0.7	-0.00114	-0.00002	0.00000	0.00000	0.00000	0.00000	0.00000	0.00000	0
0.8	-0.00019	0.00000	0.00000	0.00000	0.00000	0.00000	0.00000	0.00000	0
0.9	-0.00006	0.00000	0.00000	0.00000	0.00000	0.00000	0.00000	0.00000	0
1.0	-0.00003	0.00000	0.00000	0.00000	0.00000	0.00000	0.00000	0.00000	0
1.1	-0.00002	0.00000	0.00000	0.00000	0.00000	0.00000	0.00000	0.00000	0
1.2	0.00001	0.00000	0.00000	0.00000	0.00000	0.00000	0.00000	0.00000	0
1.3	0.00038	0.00000	0.00000	0.00000	0.00000	0.00000	0.00000	0.00000	0
1.4	0.00255	0.00011	0.00000	0.00000	0.00000	0.00000	0.00000	0.00000	0
1.5	0.01012	0.00108	0.00010	0.00001	0.00000	0.00000	0.00000	0.00000	0
1.6	0.02746	0.00649	0.00122	0.00021	0.00003	0.00001	0.00000	0.00000	0
1.7	0.05182	0.02537	0.00924	0.00297	0.00090	0.00026	0.00007	0.00002	0
1.8	0.05874	0.06132	0.04166	0.02399	0.01268	0.00636	0.00309	0.00111	0
1.9	0.01626	0.05963	0.07909	0.08186	0.07499	0.06379	0.05167	0.03349	0

because either there are ever larger compensations between one-loop and tree-level diagrams when $g_0^2 \sim 1$, or values of the coupling that are too large appear in the other cases.

The difference between the Landau and Feynman gauge results, which in absolute numbers is the same for all the actions considered (and for the plaquette action), in the case of the DBW2 gauge action, where the numbers are rather small, comes out of the same order as the results. The violations of gauge invariance are then proportionally more significant here.

All numbers that we have obtained are valid for the quenched as well as the unquenched case, because at one

loop internal quark loops can never appear in the diagrams that enter in this as well as in the other calculations presented in this paper (see Figure 1). Since the residual mass has an obvious dependence on the coupling g_0 and also depends explicitly on the value of the lattice spacing a (it is in fact given in lattice units), it is different for quenched and unquenched simulations made at the same lattice spacing, given that a and g_0 are related in a different way.

Many other general features that we have encountered in the case of the calculations made with the plaquette action are also present for improved gauge actions. Thus, the deviations from the case of exact chiral symmetry are

TABLE XV: Residual mass in lattice units at $\beta = 2.6$, in Landau gauge for the Iwasaki gauge action.

M	$N_s = 8$	$N_s = 12$	$N_s = 16$	$N_s = 20$	$N_s = 24$	$N_s = 28$	$N_s = 32$	$N_s = 48$	$N_s = \infty$
0.1	-0.26041	-0.25106	-0.22837	-0.19680	-0.16214	-0.12890	-0.09967	-0.05976	0
0.2	-0.28010	-0.17816	-0.10070	-0.05280	-0.02638	-0.01275	-0.00602	-0.00185	0
0.3	-0.18434	-0.06790	-0.02204	-0.00667	-0.00193	-0.00054	-0.00015	-0.00002	0
0.4	-0.08791	-0.01732	-0.00302	-0.00049	-0.00008	-0.00001	0.00000	0.00000	0
0.5	-0.03170	-0.00304	-0.00026	-0.00002	0.00000	0.00000	0.00000	0.00000	0
0.6	-0.00852	-0.00035	-0.00001	0.00000	0.00000	0.00000	0.00000	0.00000	0
0.7	-0.00167	-0.00003	0.00000	0.00000	0.00000	0.00000	0.00000	0.00000	0
0.8	-0.00029	0.00000	0.00000	0.00000	0.00000	0.00000	0.00000	0.00000	0
0.9	-0.00008	0.00000	0.00000	0.00000	0.00000	0.00000	0.00000	0.00000	0
1.0	-0.00004	0.00000	0.00000	0.00000	0.00000	0.00000	0.00000	0.00000	0
1.1	-0.00003	0.00000	0.00000	0.00000	0.00000	0.00000	0.00000	0.00000	0
1.2	0.00001	0.00000	0.00000	0.00000	0.00000	0.00000	0.00000	0.00000	0
1.3	0.00053	0.00001	0.00000	0.00000	0.00000	0.00000	0.00000	0.00000	0
1.4	0.00362	0.00015	0.00001	0.00000	0.00000	0.00000	0.00000	0.00000	0
1.5	0.01465	0.00152	0.00013	0.00001	0.00000	0.00000	0.00000	0.00000	0
1.6	0.04090	0.00928	0.00172	0.00029	0.00005	0.00001	0.00000	0.00000	0
1.7	0.08062	0.03709	0.01323	0.00421	0.00126	0.00036	0.00010	0.00002	0
1.8	0.10093	0.09276	0.06089	0.03453	0.01809	0.00903	0.00436	0.00157	0
1.9	0.05046	0.10077	0.12163	0.12156	0.10945	0.09220	0.07421	0.04790	0

TABLE XVI: Residual mass in lattice units at $\beta = 1.04$, in Landau gauge for the DBW2 gauge action.

M	$N_s = 8$	$N_s = 12$	$N_s = 16$	$N_s = 20$	$N_s = 24$	$N_s = 28$	$N_s = 32$	$N_s = 48$	$N_s = \infty$
0.1	-0.29645	-0.28910	-0.26373	-0.22721	-0.18696	-0.14842	-0.11460	-0.06565	0
0.2	-0.32459	-0.20788	-0.11763	-0.06168	-0.03081	-0.01489	-0.00703	-0.00198	0
0.3	-0.21621	-0.08011	-0.02607	-0.00790	-0.00229	-0.00065	-0.00018	-0.00003	0
0.4	-0.10412	-0.02066	-0.00361	-0.00059	-0.00009	-0.00001	0.00000	0.00000	0
0.5	-0.03784	-0.00366	-0.00031	-0.00002	0.00000	0.00000	0.00000	0.00000	0
0.6	-0.01022	-0.00043	-0.00002	0.00000	0.00000	0.00000	0.00000	0.00000	0
0.7	-0.00200	-0.00003	0.00000	0.00000	0.00000	0.00000	0.00000	0.00000	0
0.8	-0.00033	0.00000	0.00000	0.00000	0.00000	0.00000	0.00000	0.00000	0
0.9	-0.00009	0.00000	0.00000	0.00000	0.00000	0.00000	0.00000	0.00000	0
1.0	-0.00004	0.00000	0.00000	0.00000	0.00000	0.00000	0.00000	0.00000	0
1.1	-0.00003	0.00000	0.00000	0.00000	0.00000	0.00000	0.00000	0.00000	0
1.2	0.00001	0.00000	0.00000	0.00000	0.00000	0.00000	0.00000	0.00000	0
1.3	0.00049	0.00001	0.00000	0.00000	0.00000	0.00000	0.00000	0.00000	0
1.4	0.00336	0.00014	0.00001	0.00000	0.00000	0.00000	0.00000	0.00000	0
1.5	0.01371	0.00143	0.00013	0.00001	0.00000	0.00000	0.00000	0.00000	0
1.6	0.03866	0.00889	0.00165	0.00028	0.00005	0.00001	0.00000	0.00000	0
1.7	0.07672	0.03617	0.01301	0.00416	0.00125	0.00036	0.00010	0.00002	0
1.8	0.09526	0.09152	0.06108	0.03493	0.01839	0.00921	0.00446	0.00166	0
1.9	0.04437	0.09848	0.12253	0.12440	0.11311	0.09591	0.07755	0.05076	0

rather large when N_s is very small or M is close to 0.1 or 1.9, and, as we have seen, the residual mass is positive (with some exceptions) only when $M \gtrsim 1.2$. The rate of decay in N_s at fixed M , which is connected to the value of the mobility edge λ_c [25, 26, 27, 28, 29],

$$m_{res} \sim R_e^4 \rho_e(\lambda_c) \frac{\exp(-\lambda_c N_s)}{N_s} + R_l^4 \rho_l(0) \frac{1}{N_s} \quad (16)$$

(where ρ is the density per unit spacetime volume of the eigenvalues of the logarithm of the transfer matrix, and l and e stand for localized and extended modes with average size R respectively), increases when M grows past 1.2 and reaches a maximum before it starts to decrease,

approaching then zero near the border $M = 2$. Thus, these decays in N_s still slow down when one approaches the borders of allowed values of M ($M = 0$ and $M = 2$). This can be related to the decrease of the mobility edge λ_c towards zero in these extreme regions of M [25, 26, 27], which signals the onset of the Aoki phase. Furthermore, the phenomena happening near the borders that were discussed in [13] are also present here. Near $M = 2$ one can indeed notice that the residual mass initially grows with N_s (at fixed M) before the exponential decay finally sets in. This can be seen for example in Table VIII, where already for $M = 1.9$ the residual mass at $N_s = 12$ is larger than at $N_s = 8$, and at $N_s = 16$ is even larger.

again to Ref. [13].

IV. BILINEAR DIFFERENCES AND A POWER-DIVERGENT MIXING

Along the same lines as in [13] we have also computed the quantity $\Delta = Z_V - Z_A = -(Z_S - Z_P)/2$, which only becomes zero in the limit of infinite N_s , that is when chiral symmetry is fully restored. Since the vector and axial-vector currents renormalize differently when chiral symmetry is broken, this quantity can provide another estimate of chirality-breaking effects.

As we can gather from the results in Feynman gauge presented in Tables XIX to XXI, the amount of chirality breaking connected to Δ follows a pattern similar to the one that we have encountered in the case of the residual mass, that is Δ is relatively large for small N_s and $|1 - M|$ close to 1, and decreases when N_s grows or when $|1 - M|$ tends toward zero. As we have already remarked, the part proportional to $1 - \lambda$ of Δ is the same as for the plaquette action, which implies a violation of gauge invariance.

We can however observe here that, if one carries out comparisons at the same value of the gauge coupling, the use of improved gauge actions produces only small changes in the results for Δ compared to the plaquette action, and thus does not further suppress this quantity. When things are instead reported to the same energy scale, it is clear that the much increased value of the coupling of the DBW2 action enhances the corresponding results, and of a large factor. This is another reason to cast doubts about the adequacy of one-loop calculations in this case, as we remarked for the residual mass. In any case for the plaquette Δ was already much smaller (at given M and N_s) than m_{res} , being probably of a higher order in m_{res} as it has been suggested for four-fermion operators in [29, 30]. Looking again at the nonperturbative choice $M = 1.8$ and $N_s = 16$, the numbers that we have obtained would imply that when one increases c_1 from the plaquette to the DBW2 action the change amounts to only a few percent at most.

Thus, somewhat surprisingly, in the case of Δ improved gauge actions do not seem to make things better (at the same g_0) compared with the plaquette action. If for this quantity a reduction due to the use of improved gauge actions is evinced from numerical simulations, it should probably be traced entirely to nonperturbative effects.

We have also considered the power-divergent mixing (which is nonzero only in the case in which chiral symmetry is broken) of [31, 32]

$$O_{d_1} = \bar{q}\gamma_{[4}\gamma_5 D_{1]}q, \quad (17)$$

which is an operator related to the distribution of the (chiral even) transverse spin of quarks inside hadrons. Its mixing with an operator of lower dimension can be

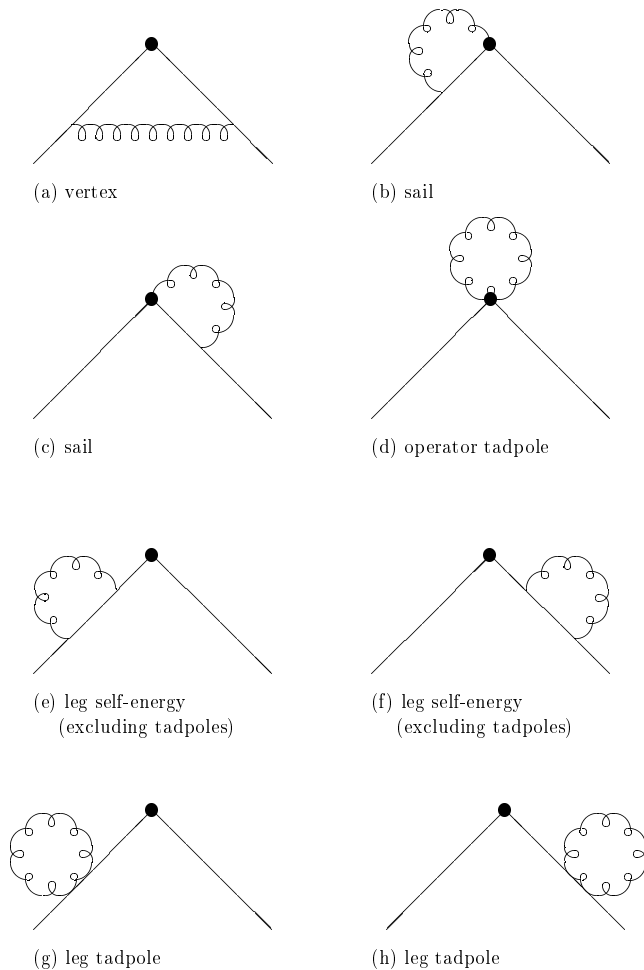


FIG. 1: The diagrams needed for the one-loop renormalization of the lattice operators.

TABLE XVII: Results for the coefficient of \bar{g}^2 of the tadpole and half-circle diagrams, for $M = 1.8$ and $N_s = 16$ in Feynman gauge, and corresponding one-loop residual mass at $\beta = 5.2$. Plaquette numbers are taken from [13]. The tree-level residual mass is also shown.

action	tadpole	half-circle	$am_{res}^{(0)}$	$am_{res}^{(1)}$
plaquette	-7.73201	0.36471	-0.01013	0.06164
Lüscher-Weisz	-6.40240	0.71569	-0.01013	0.04527
Iwasaki	-4.72902	1.22505	-0.01013	0.02400
DBW2	-3.11540	1.79449	-0.01013	0.00274

The only difference with the plaquette case is that the numbers involved are here smaller, and sometimes they can even become negative, as in the DBW2 case, however as we have already remarked in this case a two-loop calculation would likely be more appropriate.

For more discussion about these phenomena we refer

written as

$$c_{mix} \cdot \frac{i}{a} \bar{q} \sigma_{41} \gamma_5 q. \quad (18)$$

For finite N_s the results for c_{mix} in Feynman gauge are reported in Tables XXII to XXIV, where we can see that in general this mixing is almost negligible. Were this not the case, the removal of these lattice artifacts in Monte Carlo simulations of domain-wall QCD would become quite challenging.

Thus, as in the case of Δ , these chiral violations seem to be of higher order in m_{res} , and in general rather small. However here we can see that, at variance with Δ , improved gauge actions do suppress the amount of mixing (at the same g_0), with the DBW2 action producing a suppression of roughly one order of magnitude. This looks similar to what happens in the case of m_{res} . We can also notice that when c_1 increases from the Iwasaki to the DBW2 action the results happen to change sign in the region around $M = 1.8 - 1.9$, perhaps again indicating that the suppression goes too far and two-loop corrections are to be taken into account here.

We would like now to understand the different effects relative to c_{mix} and Δ that we have obtained in this Section. We can begin by noticing that, unlike the residual mass, there is no tree-level contribution to Δ and c_{mix} . Moreover, no tadpole enters in the one-loop calculations of these quantities, and certainly there cannot be any tadpole dominance here. Furthermore, still at variance with the residual mass, the half-circle diagram is also absent. In fact, in the case of Δ this diagrams cancels in the difference of V and A , while for c_{mix} it is not present from the start. Only the vertex diagram contributes then to the calculation of Δ , but in the case of c_{mix} the sail diagrams (see Figure 1) are present as well, because the operator contains a gauge field coming from the covariant derivative. This could provide the explanation for the different behaviors of Δ and c_{mix} when improved gauge actions are turned on. If one looks at the perturbative results which were obtained in the past employing improved gauge actions with Wilson [33, 34, 35] and overlap fermions [36, 37, 38, 39, 40], and also with domain-wall fermions at infinite N_s [11], one can notice that the numbers for the vertex diagrams do not change very much when going from the plaquette to improved gauge actions. For example, in the case of Wilson fermions the lattice finite constant of the vertex diagram of the vector current is 8.765394 for the plaquette action and 7.050662 for the DBW2 action. For the axial-vector current these values are 3.943879 and 5.555827 respectively. It is in general the tadpole and half-circle diagrams that end up generating the largest changes in the renormalization of these currents, but as we have remarked these diagrams do not contribute to Δ and c_{mix} .

These past results for the vertex diagrams make plausible our result that Δ is essentially not changed (at the same g_0) by the use of improved gauge actions in the case of domain-wall fermions at finite N_s . They however refer

to multiplicative renormalization factors of simple bilinear operators, and things could behave differently in the case of the power-divergent mixing coefficient c_{mix} . In looking for an explanation for the behavior of c_{mix} , we have then computed this quantity using improved gauge actions also in the case of standard Wilson fermions (for domain-wall at infinite N_s and overlap this coefficient is instead zero). To our knowledge these numbers had not been computed so far. The results of our Wilson calculations for c_{mix} are collected in Table XVIII. We have also computed it with Sheikholeslami-Wohlert fermionic improvement, and we give its numbers for $c_{sw} = 1$ and $c_{sw} = 2$, which are sufficient, since there are at most two improved vertices in the diagrams, to reconstruct c_{mix} also for any value of c_{sw} . It can then be seen that the combined use of fermionic improvement (with $c_{sw} = 1$) and improved gauge actions (especially the DBW2 action) suppresses this mixing considerably (a factor 11.25 in this case). This effect also recalls to mind what happens when UV-filtering and fermionic improvement are combined together [41]. The numbers in Table XVIII seem to make plausible the behavior of c_{mix} with improved gauge actions that we have found for domain-wall fermions at finite N_s , and in some sense the domain-wall formulation can be thought as a collection of many Wilson fermions with the appropriate damping factors. On closer inspection, it turns out that in both formulations (Wilson and domain-wall) the bulk of this decrease is produced by the sail diagrams (present here because of the covariant derivative in the operator), which then appear to be the prime responsible for the different behavior of Δ and c_{mix} .

We can also take out as a lesson from the above considerations that the effect of improved gauge actions in the case of Δ and c_{mix} remains substantially the same in the case of Wilson and domain-wall fermions.

Finally, we remark that while it is true that the combination of improved gauge actions and fermionic improvement strongly suppresses c_{mix} also in the case of the Wilson action (again, if one means that the comparisons are made at the same coupling), we should not overlook that (apart from extreme choices of N_s and M) the numbers that come out from the use of domain-wall fermions are much smaller than the ones of Wilson fermions.

TABLE XVIII: Results for the coefficient of \bar{g}^2 of c_{mix} for standard Wilson fermions (including fermionic improvement).

action	$c_{sw} = 0$	$c_{sw} = 1$	$c_{sw} = 2$
plaquette	16.243762	8.798732	0.174259
Lüscher-Weisz	13.517293	6.887859	-0.749841
Iwasaki	9.461302	4.216070	-1.756792
DBW2	4.688662	1.443948	-2.158332

TABLE XIX: Coefficient of \bar{g}^2 for the quantity $\Delta = Z_V - Z_A = -(Z_S - Z_P)/2$, in Feynman gauge for the Lüscher-Weisz gauge action.

M	$N_s = 8$	$N_s = 12$	$N_s = 16$	$N_s = 20$	$N_s = 24$	$N_s = 28$	$N_s = 32$	$N_s = 48$	$N_s = \infty$
0.1	6.6748	4.3283	2.6444	1.5535	0.8823	0.4859	0.2605	0.0178	0
0.2	2.2664	0.7107	0.1928	0.0474	0.0110	0.0024	0.0005	0.0000	0
0.3	0.5778	0.0662	0.0064	0.0006	0.0000	0.0000	0.0000	0.0000	0
0.4	0.0976	0.0034	0.0001	0.0000	0.0000	0.0000	0.0000	0.0000	0
0.5	0.0104	0.0001	0.0000	0.0000	0.0000	0.0000	0.0000	0.0000	0
0.6	0.0006	0.0000	0.0000	0.0000	0.0000	0.0000	0.0000	0.0000	0
0.7	0.0000	0.0000	0.0000	0.0000	0.0000	0.0000	0.0000	0.0000	0
0.8	0.0000	0.0000	0.0000	0.0000	0.0000	0.0000	0.0000	0.0000	0
0.9	0.0000	0.0000	0.0000	0.0000	0.0000	0.0000	0.0000	0.0000	0
1.0	0.0000	0.0000	0.0000	0.0000	0.0000	0.0000	0.0000	0.0000	0
1.1	0.0000	0.0000	0.0000	0.0000	0.0000	0.0000	0.0000	0.0000	0
1.2	0.0000	0.0000	0.0000	0.0000	0.0000	0.0000	0.0000	0.0000	0
1.3	0.0000	0.0000	0.0000	0.0000	0.0000	0.0000	0.0000	0.0000	0
1.4	0.0005	0.0000	0.0000	0.0000	0.0000	0.0000	0.0000	0.0000	0
1.5	0.0083	0.0001	0.0000	0.0000	0.0000	0.0000	0.0000	0.0000	0
1.6	0.0698	0.0029	0.0001	0.0000	0.0000	0.0000	0.0000	0.0000	0
1.7	0.3112	0.0500	0.0056	0.0005	0.0000	0.0000	0.0000	0.0000	0
1.8	0.8168	0.3640	0.1283	0.0373	0.0095	0.0022	0.0005	0.0000	0
1.9	2.1037	1.4869	1.0150	0.6819	0.4453	0.2795	0.1679	0.0152	0

 TABLE XX: Coefficient of \bar{g}^2 for the quantity $\Delta = Z_V - Z_A = -(Z_S - Z_P)/2$, in Feynman gauge for the Iwasaki gauge action.

M	$N_s = 8$	$N_s = 12$	$N_s = 16$	$N_s = 20$	$N_s = 24$	$N_s = 28$	$N_s = 32$	$N_s = 48$	$N_s = \infty$
0.1	6.2243	4.1314	2.5590	1.5166	0.8664	0.4791	0.2575	0.0177	0
0.2	2.1620	0.6927	0.1897	0.0469	0.0109	0.0024	0.0005	0.0000	0
0.3	0.5578	0.0650	0.0063	0.0006	0.0000	0.0000	0.0000	0.0000	0
0.4	0.0945	0.0033	0.0001	0.0000	0.0000	0.0000	0.0000	0.0000	0
0.5	0.0100	0.0001	0.0000	0.0000	0.0000	0.0000	0.0000	0.0000	0
0.6	0.0006	0.0000	0.0000	0.0000	0.0000	0.0000	0.0000	0.0000	0
0.7	0.0000	0.0000	0.0000	0.0000	0.0000	0.0000	0.0000	0.0000	0
0.8	0.0000	0.0000	0.0000	0.0000	0.0000	0.0000	0.0000	0.0000	0
0.9	0.0000	0.0000	0.0000	0.0000	0.0000	0.0000	0.0000	0.0000	0
1.0	0.0000	0.0000	0.0000	0.0000	0.0000	0.0000	0.0000	0.0000	0
1.1	0.0000	0.0000	0.0000	0.0000	0.0000	0.0000	0.0000	0.0000	0
1.2	0.0000	0.0000	0.0000	0.0000	0.0000	0.0000	0.0000	0.0000	0
1.3	0.0000	0.0000	0.0000	0.0000	0.0000	0.0000	0.0000	0.0000	0
1.4	0.0005	0.0000	0.0000	0.0000	0.0000	0.0000	0.0000	0.0000	0
1.5	0.0082	0.0001	0.0000	0.0000	0.0000	0.0000	0.0000	0.0000	0
1.6	0.0694	0.0029	0.0001	0.0000	0.0000	0.0000	0.0000	0.0000	0
1.7	0.3073	0.0497	0.0056	0.0005	0.0000	0.0000	0.0000	0.0000	0
1.8	0.7891	0.3592	0.1275	0.0372	0.0095	0.0022	0.0005	0.0000	0
1.9	1.9492	1.4179	0.9846	0.6686	0.4396	0.2770	0.1668	0.0152	0

V. CONCLUSIONS

In this article we have presented the calculations of a few one-loop amplitudes for domain-wall fermions at finite N_s using improved gauge actions, with the intention of studying in perturbation theory the phenomenon of reduction of chiral violations associated with these gauge actions. In particular, we have considered three quantities whose differences from their (vanishing) values at $N_s = \infty$ can provide some significant estimates of chiral violations: the residual mass, the difference Δ between

the vector and axial-vector renormalization constants, and c_{mix} , a power-divergent mixing of a deep-inelastic operator which is entirely due to the breaking of chirality.

It is then useful to compare the results presented in this paper with the ones computed in Ref. [13] for the simple plaquette action, and see whether and how much they have decreased when the coupling is kept constant. Our calculations show that also in the framework of one-loop perturbation theory the use of improved gauge actions can indeed suppress the residual mass. The largest sup-

TABLE XXI: Coefficient of \bar{g}^2 for the quantity $\Delta = Z_V - Z_A = -(Z_S - Z_P)/2$, in Feynman gauge for the DBW2 gauge action.

M	$N_s = 8$	$N_s = 12$	$N_s = 16$	$N_s = 20$	$N_s = 24$	$N_s = 28$	$N_s = 32$	$N_s = 48$	$N_s = \infty$
0.1	5.4947	3.8063	2.4168	1.4548	0.8396	0.4675	0.2525	0.0175	0
0.2	1.9894	0.6623	0.1845	0.0460	0.0108	0.0024	0.0005	0.0000	0
0.3	0.5250	0.0629	0.0062	0.0005	0.0000	0.0000	0.0000	0.0000	0
0.4	0.0896	0.0032	0.0001	0.0000	0.0000	0.0000	0.0000	0.0000	0
0.5	0.0094	0.0001	0.0000	0.0000	0.0000	0.0000	0.0000	0.0000	0
0.6	0.0005	0.0000	0.0000	0.0000	0.0000	0.0000	0.0000	0.0000	0
0.7	0.0000	0.0000	0.0000	0.0000	0.0000	0.0000	0.0000	0.0000	0
0.8	0.0000	0.0000	0.0000	0.0000	0.0000	0.0000	0.0000	0.0000	0
0.9	0.0000	0.0000	0.0000	0.0000	0.0000	0.0000	0.0000	0.0000	0
1.0	0.0000	0.0000	0.0000	0.0000	0.0000	0.0000	0.0000	0.0000	0
1.1	0.0000	0.0000	0.0000	0.0000	0.0000	0.0000	0.0000	0.0000	0
1.2	0.0000	0.0000	0.0000	0.0000	0.0000	0.0000	0.0000	0.0000	0
1.3	0.0000	0.0000	0.0000	0.0000	0.0000	0.0000	0.0000	0.0000	0
1.4	0.0005	0.0000	0.0000	0.0000	0.0000	0.0000	0.0000	0.0000	0
1.5	0.0082	0.0001	0.0000	0.0000	0.0000	0.0000	0.0000	0.0000	0
1.6	0.0688	0.0029	0.0001	0.0000	0.0000	0.0000	0.0000	0.0000	0
1.7	0.3021	0.0494	0.0055	0.0005	0.0000	0.0000	0.0000	0.0000	0
1.8	0.7516	0.3521	0.1262	0.0369	0.0095	0.0022	0.0005	0.0000	0
1.9	1.7396	1.3168	0.9384	0.6480	0.4305	0.2730	0.1651	0.0151	0

TABLE XXII: Coefficient of \bar{g}^2 for the coefficient of the power-divergent mixing of O_{d_1} , c_{mix} in Eq. (18), in Feynman gauge for the Lüscher-Weisz gauge action.

M	$N_s = 8$	$N_s = 12$	$N_s = 16$	$N_s = 20$	$N_s = 24$	$N_s = 28$	$N_s = 32$	$N_s = 48$	$N_s = \infty$
0.1	-12.2811	-7.3668	-4.6923	-3.0533	-2.0014	-1.3145	-0.8635	-0.1604	0
0.2	-5.0766	-2.1043	-0.8697	-0.3578	-0.1471	-0.0605	-0.0249	-0.0007	0
0.3	-2.1594	-0.5314	-0.1293	-0.0315	-0.0077	-0.0019	-0.0005	0.0000	0
0.4	-0.8140	-0.1104	-0.0148	-0.0020	-0.0003	0.0000	0.0000	0.0000	0
0.5	-0.2675	-0.0186	-0.0012	-0.0001	0.0000	0.0000	0.0000	0.0000	0
0.6	-0.0768	-0.0025	-0.0001	0.0000	0.0000	0.0000	0.0000	0.0000	0
0.7	-0.0197	-0.0003	0.0000	0.0000	0.0000	0.0000	0.0000	0.0000	0
0.8	-0.0050	-0.0001	0.0000	0.0000	0.0000	0.0000	0.0000	0.0000	0
0.9	-0.0013	0.0000	0.0000	0.0000	0.0000	0.0000	0.0000	0.0000	0
1.0	0.0000	0.0000	0.0000	0.0000	0.0000	0.0000	0.0000	0.0000	0
1.1	0.0006	0.0000	0.0000	0.0000	0.0000	0.0000	0.0000	0.0000	0
1.2	0.0011	0.0000	0.0000	0.0000	0.0000	0.0000	0.0000	0.0000	0
1.3	0.0024	0.0000	0.0000	0.0000	0.0000	0.0000	0.0000	0.0000	0
1.4	0.0097	0.0002	0.0000	0.0000	0.0000	0.0000	0.0000	0.0000	0
1.5	0.0409	0.0021	0.0001	0.0000	0.0000	0.0000	0.0000	0.0000	0
1.6	0.1467	0.0142	0.0015	0.0002	0.0000	0.0000	0.0000	0.0000	0
1.7	0.4250	0.0767	0.0142	0.0028	0.0006	0.0001	0.0000	0.0000	0
1.8	0.9787	0.3200	0.1056	0.0345	0.0113	0.0038	0.0013	0.0000	0
1.9	1.8728	0.9467	0.5303	0.3068	0.1790	0.1043	0.0605	0.0064	0

pressions are produced by the DBW2 action, and this dramatic decrease, of about one order of magnitude, is due to the combined effects of the changes in the (order-zero) tadpole and half-circle diagrams of the self-energy. Thus, our perturbative results, when used at the same values of g_0 for the various actions, may qualitatively confirm what is known from Monte Carlo simulations about the consequences of using improved gauge actions.

On the other hand, if one compares the various actions at the same energy scale, perturbation theory gives rather puzzling results (especially in the case of the DBW2 ac-

tion), and its use appears to be problematic (at least at the one-loop level), also because of the large values that the gauge coupling assumes at the scale of 2 GeV.

We have also found that the effects of improved gauge actions can also be different depending on the quantity studied. When g_0 is kept fixed, there is indeed a dramatic suppression of the residual mass and of the power-divergent mixing coefficient c_{mix} for the DBW2 action, whereas for Δ only very small changes are observed when instead of the plaquette any of the improved gauge actions is used. A lesson from this could be that some (but

TABLE XXIII: Coefficient of \bar{g}^2 for the coefficient of the power-divergent mixing of O_{d_1} , c_{mix} in Eq. (18), in Feynman gauge for the Iwasaki gauge action.

M	$N_s = 8$	$N_s = 12$	$N_s = 16$	$N_s = 20$	$N_s = 24$	$N_s = 28$	$N_s = 32$	$N_s = 48$	$N_s = \infty$
0.1	-9.4574	-5.7117	-3.6538	-2.3844	-1.5659	-1.0297	-0.6769	-0.1259	0
0.2	-3.9356	-1.6453	-0.6821	-0.2810	-0.1156	-0.0476	-0.0196	-0.0006	0
0.3	-1.6731	-0.4139	-0.1010	-0.0247	-0.0060	-0.0015	-0.0004	0.0000	0
0.4	-0.6240	-0.0853	-0.0115	-0.0015	-0.0002	0.0000	0.0000	0.0000	0
0.5	-0.2020	-0.0142	-0.0010	-0.0001	0.0000	0.0000	0.0000	0.0000	0
0.6	-0.0570	-0.0019	-0.0001	0.0000	0.0000	0.0000	0.0000	0.0000	0
0.7	-0.0143	-0.0002	0.0000	0.0000	0.0000	0.0000	0.0000	0.0000	0
0.8	-0.0035	0.0000	0.0000	0.0000	0.0000	0.0000	0.0000	0.0000	0
0.9	-0.0009	0.0000	0.0000	0.0000	0.0000	0.0000	0.0000	0.0000	0
1.0	0.0000	0.0000	0.0000	0.0000	0.0000	0.0000	0.0000	0.0000	0
1.1	0.0004	0.0000	0.0000	0.0000	0.0000	0.0000	0.0000	0.0000	0
1.2	0.0007	0.0000	0.0000	0.0000	0.0000	0.0000	0.0000	0.0000	0
1.3	0.0015	0.0000	0.0000	0.0000	0.0000	0.0000	0.0000	0.0000	0
1.4	0.0054	0.0001	0.0000	0.0000	0.0000	0.0000	0.0000	0.0000	0
1.5	0.0218	0.0009	0.0000	0.0000	0.0000	0.0000	0.0000	0.0000	0
1.6	0.0773	0.0053	0.0004	0.0000	0.0000	0.0000	0.0000	0.0000	0
1.7	0.2172	0.0273	0.0024	-0.0001	-0.0001	0.0000	0.0000	0.0000	0
1.8	0.4328	0.1029	0.0172	-0.0016	-0.0035	-0.0023	-0.0012	0.0000	0
1.9	0.4010	0.0932	-0.0035	-0.0366	-0.0444	-0.0417	-0.0352	-0.0113	0

TABLE XXIV: Coefficient of \bar{g}^2 for the coefficient of the power-divergent mixing of O_{d_1} , c_{mix} in Eq. (18), in Feynman gauge for the DBW2 gauge action.

M	$N_s = 8$	$N_s = 12$	$N_s = 16$	$N_s = 20$	$N_s = 24$	$N_s = 28$	$N_s = 32$	$N_s = 48$	$N_s = \infty$
0.1	-5.8666	-3.5954	-2.3230	-1.5265	-1.0072	-0.6642	-0.4374	-0.0815	0
0.2	-2.4673	-1.0511	-0.4388	-0.1812	-0.0747	-0.0308	-0.0128	-0.0004	0
0.3	-1.0435	-0.2604	-0.0639	-0.0157	-0.0039	-0.0010	-0.0002	0.0000	0
0.4	-0.3771	-0.0521	-0.0072	-0.0010	-0.0001	0.0000	0.0000	0.0000	0
0.5	-0.1165	-0.0084	-0.0006	0.0000	0.0000	0.0000	0.0000	0.0000	0
0.6	-0.0313	-0.0011	0.0000	0.0000	0.0000	0.0000	0.0000	0.0000	0
0.7	-0.0074	-0.0001	0.0000	0.0000	0.0000	0.0000	0.0000	0.0000	0
0.8	-0.0017	0.0000	0.0000	0.0000	0.0000	0.0000	0.0000	0.0000	0
0.9	-0.0004	0.0000	0.0000	0.0000	0.0000	0.0000	0.0000	0.0000	0
1.0	0.0000	0.0000	0.0000	0.0000	0.0000	0.0000	0.0000	0.0000	0
1.1	0.0002	0.0000	0.0000	0.0000	0.0000	0.0000	0.0000	0.0000	0
1.2	0.0003	0.0000	0.0000	0.0000	0.0000	0.0000	0.0000	0.0000	0
1.3	0.0005	0.0000	0.0000	0.0000	0.0000	0.0000	0.0000	0.0000	0
1.4	0.0011	0.0000	0.0000	0.0000	0.0000	0.0000	0.0000	0.0000	0
1.5	0.0030	-0.0002	0.0000	0.0000	0.0000	0.0000	0.0000	0.0000	0
1.6	0.0115	-0.0031	-0.0007	-0.0001	0.0000	0.0000	0.0000	0.0000	0
1.7	0.0279	-0.0171	-0.0082	-0.0026	-0.0007	-0.0002	0.0000	0.0000	0
1.8	-0.0434	-0.0836	-0.0583	-0.0325	-0.0161	-0.0074	-0.0033	-0.0001	0
1.9	-0.8296	-0.6069	-0.4382	-0.3152	-0.2253	-0.1599	-0.1125	-0.0256	0

by no means not all) quantities which measure chiral violations but are of higher order in m_{res} will get little or no reduction even with improved gauge actions.

reminding me to compare the various actions at their proper values of β .

Acknowledgments

I am grateful for the support by Fonds zur Förderung der Wissenschaftlichen Forschung in Österreich (FWF), Project P16310-N08. I also thank Rainer Sommer for

APPENDIX: SOME PLAQUETTE RESULTS

In this Appendix we collect some useful reference results derived in [13] for the plaquette action. Values of the tree-level residual mass (valid for any kind of gluon action) are reported in Table XXV. The plaquette num-

bers for Σ_0 in Feynman gauge are shown in Table XXVI, and the corresponding one-loop residual mass for $\beta = 5.2$ and $\beta = 6.0$ in Landau gauge are reported in Tables XXVII and XXVIII.

The plaquette numbers for Δ and c_{mix} in Feynman gauge are finally shown in Tables XXIX and XXX respectively.

-
- [1] K. Orginos [RBC Collaboration], Nucl. Phys. Proc. Suppl. **106**, 721 (2002) [arXiv:hep-lat/0110074].
- [2] Y. Aoki *et al.*, Phys. Rev. D **69**, 074504 (2004) [arXiv:hep-lat/0211023].
- [3] Y. Aoki *et al.*, Phys. Rev. D **73**, 094507 (2006) [arXiv:hep-lat/0508011].
- [4] F. Berruto, T. Blum, K. Orginos and A. Soni, Phys. Rev. D **73**, 054509 (2006) [arXiv:hep-lat/0512004].
- [5] Y. Aoki, C. Dawson, J. Noaki and A. Soni, arXiv:hep-lat/0607002.
- [6] P. A. Boyle, M. A. Donnellan, J. M. Flynn, A. Jüttner, J. Noaki, C. T. Sachrajda and R. J. Tweedie [UKQCD Collaboration], arXiv:hep-lat/0607018.
- [7] H. W. Lin, S. Ohta and N. Yamada [RBC Collaboration], Nucl. Phys. Proc. Suppl. **153**, 199 (2006).
- [8] H. W. Lin, S. Ohta, A. Soni and N. Yamada, arXiv:hep-lat/0607035.
- [9] C. Dawson, T. Izubuchi, T. Kaneko, S. Sasaki and A. Soni, arXiv:hep-ph/0607162.
- [10] K. Orginos, plenary talk at the Lattice 2006 International Symposium, Tucson (AZ), to be published in PoS **LAT2006**.
- [11] S. Aoki, T. Izubuchi, Y. Kuramashi and Y. Taniguchi, Phys. Rev. D **67**, 094502 (2003) [arXiv:hep-lat/0206013].
- [12] Y. Nakamura and Y. Kuramashi, Phys. Rev. D **73**, 094502 (2006) [arXiv:hep-lat/0603012].
- [13] S. Capitani, arXiv:hep-lat/0606022.
- [14] M. Lüscher and P. Weisz, Commun. Math. Phys. **97**, 59 (1985) [Erratum-ibid. **98**, 433 (1985)].
- [15] Y. Iwasaki, UTHEP-118.
- [16] T. Takaishi, Phys. Rev. D **54**, 1050 (1996).
- [17] P. de Forcrand *et al.* [QCD-TARO Collaboration], Nucl. Phys. B **577**, 263 (2000) [arXiv:hep-lat/9911033].
- [18] Y. Shamir, Nucl. Phys. B **406**, 90 (1993) [arXiv:hep-lat/9303005].
- [19] P. Weisz and R. Wohlert, Nucl. Phys. B **236**, 397 (1984) [Erratum-ibid. B **247**, 544 (1984)].
- [20] J. A. M. Vermaseren, arXiv:math-ph/0010025.
- [21] P. M. Vranas, Phys. Rev. D **57**, 1415 (1998) [arXiv:hep-lat/9705023].
- [22] P. M. Vranas, Nucl. Phys. Proc. Suppl. **63**, 605 (1998) [arXiv:hep-lat/9709119].
- [23] S. Aoki, T. Izubuchi, Y. Kuramashi and Y. Taniguchi, Phys. Rev. D **59**, 094505 (1999) [arXiv:hep-lat/9810020].
- [24] S. Capitani, Phys. Rept. **382**, 113 (2003) [arXiv:hep-lat/0211036].
- [25] M. Golterman and Y. Shamir, Phys. Rev. D **68**, 074501 (2003) [arXiv:hep-lat/0306002].
- [26] M. Golterman, Y. Shamir and B. Svetitsky, Phys. Rev. D **71**, 071502 (2005) [arXiv:hep-lat/0407021].
- [27] M. Golterman, Y. Shamir and B. Svetitsky, Phys. Rev. D **72**, 034501 (2005) [arXiv:hep-lat/0503037].
- [28] B. Svetitsky, Y. Shamir and M. Golterman, PoS **LAT2005**, 129 (2005) [arXiv:hep-lat/0508015].
- [29] N. Christ [RBC and UKQCD Collaborations], PoS **LAT2005**, 345 (2005).
- [30] Y. Aoki *et al.*, Phys. Rev. D **72**, 114505 (2005) [arXiv:hep-lat/0411006].
- [31] S. Capitani, Nucl. Phys. B **597**, 313 (2001) [arXiv:hep-lat/0009018].
- [32] S. Capitani, Phys. Rev. D **73**, 014505 (2006) [arXiv:hep-lat/0510091].
- [33] S. Aoki, K. i. Nagai, Y. Taniguchi and A. Ukawa, Phys. Rev. D **58**, 074505 (1998) [arXiv:hep-lat/9802034].
- [34] Y. Taniguchi, S. Aoki, K. i. Nagai and A. Ukawa, Nucl. Phys. Proc. Suppl. **73**, 912 (1999) [arXiv:hep-lat/9809070].
- [35] S. Aoki, Y. Kuramashi, T. Onogi and N. Tsutsui, Int. J. Mod. Phys. A **15**, 3521 (2000) [arXiv:hep-lat/0001005].
- [36] R. Horsley, H. Perlt, P. E. L. Rakow, G. Schierholz and A. Schiller [QCDSF Collaboration], Nucl. Phys. B **693**, 3 (2004) [Erratum-ibid. B **713**, 601 (2005)] [arXiv:hep-lat/0404007].
- [37] R. Horsley, H. Perlt, P. E. L. Rakow, G. Schierholz and A. Schiller [QCDSF Collaboration], Phys. Lett. B **628**, 66 (2005) [arXiv:hep-lat/0505015].
- [38] R. Horsley, H. Perlt, P. E. L. Rakow, G. Schierholz and A. Schiller, PoS **LAT2005**, 238 (2006) [arXiv:hep-lat/0509072].
- [39] M. Ioannou and H. Panagopoulos, PoS **LAT2005**, 229 (2006) [arXiv:hep-lat/0512039].
- [40] M. Ioannou and H. Panagopoulos, Phys. Rev. D **73**, 054507 (2006) [arXiv:hep-lat/0601020].
- [41] S. Capitani, S. Dürr and C. Hoelbling, arXiv:hep-lat/0607006.

TABLE XXV: Residual mass at tree level in lattice units (multiplied for $16\pi^2$).

M	$N_s = 8$	$N_s = 12$	$N_s = 16$	$N_s = 20$	$N_s = 24$	$N_s = 28$	$N_s = 32$	$N_s = 48$	$N_s = \infty$
0.1	-12.91556	-8.47390	-5.55973	-3.64774	-2.39328	-1.57023	-1.03023	-0.19090	0
0.2	-9.53767	-3.90663	-1.60015	-0.65542	-0.26846	-0.10996	-0.04504	-0.00127	0
0.3	-4.64274	-1.11472	-0.26764	-0.06426	-0.01543	-0.00370	-0.00089	0.00000	0
0.4	-1.69750	-0.22000	-0.02851	-0.00370	-0.00048	-0.00006	-0.00001	0.00000	0
0.5	-0.46264	-0.02891	-0.00181	-0.00011	-0.00001	0.00000	0.00000	0.00000	0
0.6	-0.08693	-0.00223	-0.00006	0.00000	0.00000	0.00000	0.00000	0.00000	0
0.7	-0.00943	-0.00008	0.00000	0.00000	0.00000	0.00000	0.00000	0.00000	0
0.8	-0.00039	0.00000	0.00000	0.00000	0.00000	0.00000	0.00000	0.00000	0
0.9	0.00000	0.00000	0.00000	0.00000	0.00000	0.00000	0.00000	0.00000	0
1.0	0.00000	0.00000	0.00000	0.00000	0.00000	0.00000	0.00000	0.00000	0
1.1	0.00000	0.00000	0.00000	0.00000	0.00000	0.00000	0.00000	0.00000	0
1.2	-0.00039	0.00000	0.00000	0.00000	0.00000	0.00000	0.00000	0.00000	0
1.3	-0.00943	-0.00008	0.00000	0.00000	0.00000	0.00000	0.00000	0.00000	0
1.4	-0.08693	-0.00223	-0.00006	0.00000	0.00000	0.00000	0.00000	0.00000	0
1.5	-0.46264	-0.02891	-0.00181	-0.00011	-0.00001	0.00000	0.00000	0.00000	0
1.6	-1.69750	-0.22000	-0.02851	-0.00370	-0.00048	-0.00006	-0.00001	0.00000	0
1.7	-4.64274	-1.11472	-0.26764	-0.06426	-0.01543	-0.00370	-0.00089	0.00000	0
1.8	-9.53767	-3.90663	-1.60015	-0.65542	-0.26846	-0.10996	-0.04504	-0.00127	0
1.9	-12.91556	-8.47390	-5.55973	-3.64774	-2.39328	-1.57023	-1.03023	-0.19090	0

TABLE XXVI: Coefficient of g^2 for the complete result of Σ_0 , in Feynman gauge for the plaquette gauge action.

M	$N_s = 8$	$N_s = 12$	$N_s = 16$	$N_s = 20$	$N_s = 24$	$N_s = 28$	$N_s = 32$	$N_s = 48$	$N_s = \infty$
0.1	17.85919	19.67880	19.25277	17.32109	14.66546	11.87550	9.30218	2.86309	0
0.2	21.82264	15.20660	8.97397	4.82019	2.44504	1.19446	0.56831	0.02488	0
0.3	15.28940	5.98758	1.99997	0.61538	0.18022	0.05106	0.01412	0.00007	0
0.4	7.55847	1.55410	0.27613	0.04548	0.00713	0.00108	0.00016	0.00000	0
0.5	2.79190	0.27543	0.02358	0.00186	0.00014	0.00001	0.00000	0.00000	0
0.6	0.76252	0.03191	0.00115	0.00004	0.00000	0.00000	0.00000	0.00000	0
0.7	0.15015	0.00250	0.00004	0.00000	0.00000	0.00000	0.00000	0.00000	0
0.8	0.02561	0.00031	0.00001	0.00000	0.00000	0.00000	0.00000	0.00000	0
0.9	0.00774	0.00012	0.00000	0.00000	0.00000	0.00000	0.00000	0.00000	0
1.0	0.00418	0.00008	0.00000	0.00000	0.00000	0.00000	0.00000	0.00000	0
1.1	0.00283	0.00007	0.00000	0.00000	0.00000	0.00000	0.00000	0.00000	0
1.2	-0.00172	0.00006	0.00000	0.00000	0.00000	0.00000	0.00000	0.00000	0
1.3	-0.06252	-0.00073	0.00000	0.00000	0.00000	0.00000	0.00000	0.00000	0
1.4	-0.44327	-0.01733	-0.00060	-0.00002	0.00000	0.00000	0.00000	0.00000	0
1.5	-1.85863	-0.18051	-0.01531	-0.00122	-0.00009	-0.00001	0.00000	0.00000	0
1.6	-5.42629	-1.12306	-0.20001	-0.03298	-0.00521	-0.00080	-0.00012	0.00000	0
1.7	-11.49207	-4.61264	-1.55867	-0.48269	-0.14194	-0.04034	-0.01120	-0.00006	0
1.8	-16.77186	-12.20090	-7.36730	-4.00994	-2.05105	-1.00765	-0.48138	-0.02129	0
1.9	-13.69620	-15.97157	-16.18935	-14.90821	-12.82561	-10.50396	-8.29629	-2.59956	0

TABLE XXVII: Residual mass in lattice units at $\beta = 5.2$, in Landau gauge for the plaquette gauge action.

M	$N_s = 8$	$N_s = 12$	$N_s = 16$	$N_s = 20$	$N_s = 24$	$N_s = 28$	$N_s = 32$	$N_s = 48$	$N_s = \infty$
0.1	-0.25014	-0.24077	-0.21923	-0.18923	-0.15614	-0.12430	-0.09621	-0.02889	0
0.2	-0.26738	-0.17001	-0.09619	-0.05047	-0.02523	-0.01220	-0.00576	-0.00025	0
0.3	-0.17502	-0.06438	-0.02089	-0.00632	-0.00183	-0.00051	-0.00014	0.00000	0
0.4	-0.08294	-0.01629	-0.00283	-0.00046	-0.00007	-0.00001	0.00000	0.00000	0
0.5	-0.02966	-0.00283	-0.00024	-0.00002	0.00000	0.00000	0.00000	0.00000	0
0.6	-0.00787	-0.00032	-0.00001	0.00000	0.00000	0.00000	0.00000	0.00000	0
0.7	-0.00151	-0.00002	0.00000	0.00000	0.00000	0.00000	0.00000	0.00000	0
0.8	-0.00025	0.00000	0.00000	0.00000	0.00000	0.00000	0.00000	0.00000	0
0.9	-0.00008	0.00000	0.00000	0.00000	0.00000	0.00000	0.00000	0.00000	0
1.0	-0.00004	0.00000	0.00000	0.00000	0.00000	0.00000	0.00000	0.00000	0
1.1	-0.00003	0.00000	0.00000	0.00000	0.00000	0.00000	0.00000	0.00000	0
1.2	0.00002	0.00000	0.00000	0.00000	0.00000	0.00000	0.00000	0.00000	0
1.3	0.00056	0.00001	0.00000	0.00000	0.00000	0.00000	0.00000	0.00000	0
1.4	0.00387	0.00016	0.00001	0.00000	0.00000	0.00000	0.00000	0.00000	0
1.5	0.01565	0.00161	0.00014	0.00001	0.00000	0.00000	0.00000	0.00000	0
1.6	0.04357	0.00979	0.00181	0.00030	0.00005	0.00001	0.00000	0.00000	0
1.7	0.08592	0.03889	0.01378	0.00438	0.00131	0.00038	0.00011	0.00000	0
1.8	0.10875	0.09702	0.06302	0.03555	0.01857	0.00925	0.00446	0.00020	0
1.9	0.05763	0.10669	0.12612	0.12479	0.11169	0.09373	0.07524	0.02433	0

TABLE XXVIII: Residual mass in lattice units at $\beta = 6$, in Landau gauge for the plaquette gauge action.

M	$N_s = 8$	$N_s = 12$	$N_s = 16$	$N_s = 20$	$N_s = 24$	$N_s = 28$	$N_s = 32$	$N_s = 48$	$N_s = \infty$
0.1	-0.22770	-0.21582	-0.19469	-0.16708	-0.13735	-0.10905	-0.08425	-0.02520	0
0.2	-0.23978	-0.15064	-0.08471	-0.04430	-0.02209	-0.01067	-0.00503	-0.00022	0
0.3	-0.15560	-0.05674	-0.01833	-0.00553	-0.00160	-0.00045	-0.00012	0.00000	0
0.4	-0.07331	-0.01430	-0.00248	-0.00040	-0.00006	-0.00001	0.00000	0.00000	0
0.5	-0.02610	-0.00247	-0.00021	-0.00002	0.00000	0.00000	0.00000	0.00000	0
0.6	-0.00690	-0.00028	-0.00001	0.00000	0.00000	0.00000	0.00000	0.00000	0
0.7	-0.00132	-0.00002	0.00000	0.00000	0.00000	0.00000	0.00000	0.00000	0
0.8	-0.00022	0.00000	0.00000	0.00000	0.00000	0.00000	0.00000	0.00000	0
0.9	-0.00007	0.00000	0.00000	0.00000	0.00000	0.00000	0.00000	0.00000	0
1.0	-0.00004	0.00000	0.00000	0.00000	0.00000	0.00000	0.00000	0.00000	0
1.1	-0.00002	0.00000	0.00000	0.00000	0.00000	0.00000	0.00000	0.00000	0
1.2	0.00001	0.00000	0.00000	0.00000	0.00000	0.00000	0.00000	0.00000	0
1.3	0.00048	0.00001	0.00000	0.00000	0.00000	0.00000	0.00000	0.00000	0
1.4	0.00328	0.00014	0.00000	0.00000	0.00000	0.00000	0.00000	0.00000	0
1.5	0.01317	0.00137	0.00012	0.00001	0.00000	0.00000	0.00000	0.00000	0
1.6	0.03632	0.00830	0.00154	0.00026	0.00004	0.00001	0.00000	0.00000	0
1.7	0.07054	0.03276	0.01172	0.00374	0.00112	0.00032	0.00009	0.00000	0
1.8	0.08620	0.08078	0.05326	0.03026	0.01587	0.00793	0.00383	0.00017	0
1.9	0.03905	0.08531	0.10461	0.10507	0.09478	0.07991	0.06434	0.02093	0

TABLE XXIX: Coefficient of \bar{g}^2 for Δ , in Feynman gauge for the plaquette gauge action.

M	$N_s = 8$	$N_s = 12$	$N_s = 16$	$N_s = 20$	$N_s = 24$	$N_s = 28$	$N_s = 32$	$N_s = 48$	$N_s = \infty$
0.1	6.9399	4.4434	2.6941	1.5749	0.8916	0.4899	0.2622	0.0179	0
0.2	2.3272	0.7211	0.1945	0.0477	0.0110	0.0025	0.0005	0.0000	0
0.3	0.5894	0.0668	0.0064	0.0006	0.0000	0.0000	0.0000	0.0000	0
0.4	0.0994	0.0034	0.0001	0.0000	0.0000	0.0000	0.0000	0.0000	0
0.5	0.0106	0.0001	0.0000	0.0000	0.0000	0.0000	0.0000	0.0000	0
0.6	0.0007	0.0000	0.0000	0.0000	0.0000	0.0000	0.0000	0.0000	0
0.7	0.0000	0.0000	0.0000	0.0000	0.0000	0.0000	0.0000	0.0000	0
0.8	0.0000	0.0000	0.0000	0.0000	0.0000	0.0000	0.0000	0.0000	0
0.9	0.0000	0.0000	0.0000	0.0000	0.0000	0.0000	0.0000	0.0000	0
1.0	0.0000	0.0000	0.0000	0.0000	0.0000	0.0000	0.0000	0.0000	0
1.1	0.0000	0.0000	0.0000	0.0000	0.0000	0.0000	0.0000	0.0000	0
1.2	0.0000	0.0000	0.0000	0.0000	0.0000	0.0000	0.0000	0.0000	0
1.3	0.0000	0.0000	0.0000	0.0000	0.0000	0.0000	0.0000	0.0000	0
1.4	0.0005	0.0000	0.0000	0.0000	0.0000	0.0000	0.0000	0.0000	0
1.5	0.0083	0.0001	0.0000	0.0000	0.0000	0.0000	0.0000	0.0000	0
1.6	0.0701	0.0029	0.0001	0.0000	0.0000	0.0000	0.0000	0.0000	0
1.7	0.3140	0.0501	0.0056	0.0005	0.0000	0.0000	0.0000	0.0000	0
1.8	0.8354	0.3672	0.1288	0.0374	0.0096	0.0022	0.0005	0.0000	0
1.9	2.2075	1.5323	1.0348	0.6904	0.4490	0.2811	0.1686	0.0153	0

TABLE XXX: Coefficient of \bar{g}^2 for c_{mix} , in Feynman gauge for the plaquette gauge action.

M	$N_s = 8$	$N_s = 12$	$N_s = 16$	$N_s = 20$	$N_s = 24$	$N_s = 28$	$N_s = 32$	$N_s = 48$	$N_s = \infty$
0.1	-14.1244	-8.4448	-5.3682	-3.4884	-2.2846	-1.4996	-0.9848	-0.1829	0
0.2	-5.8166	-2.4014	-0.9910	-0.4075	-0.1674	-0.0688	-0.0283	-0.0008	0
0.3	-2.4733	-0.6070	-0.1475	-0.0359	-0.0087	-0.0021	-0.0005	0.0000	0
0.4	-0.9361	-0.1265	-0.0169	-0.0022	-0.0003	0.0000	0.0000	0.0000	0
0.5	-0.3094	-0.0213	-0.0014	-0.0001	0.0000	0.0000	0.0000	0.0000	0
0.6	-0.0893	-0.0029	-0.0001	0.0000	0.0000	0.0000	0.0000	0.0000	0
0.7	-0.0231	-0.0004	0.0000	0.0000	0.0000	0.0000	0.0000	0.0000	0
0.8	-0.0059	-0.0001	0.0000	0.0000	0.0000	0.0000	0.0000	0.0000	0
0.9	-0.0015	0.0000	0.0000	0.0000	0.0000	0.0000	0.0000	0.0000	0
1.0	0.0000	0.0000	0.0000	0.0000	0.0000	0.0000	0.0000	0.0000	0
1.1	0.0008	0.0000	0.0000	0.0000	0.0000	0.0000	0.0000	0.0000	0
1.2	0.0014	0.0000	0.0000	0.0000	0.0000	0.0000	0.0000	0.0000	0
1.3	0.0031	0.0001	0.0000	0.0000	0.0000	0.0000	0.0000	0.0000	0
1.4	0.0127	0.0003	0.0000	0.0000	0.0000	0.0000	0.0000	0.0000	0
1.5	0.0546	0.0029	0.0002	0.0000	0.0000	0.0000	0.0000	0.0000	0
1.6	0.1969	0.0207	0.0024	0.0003	0.0000	0.0000	0.0000	0.0000	0
1.7	0.5774	0.1129	0.0229	0.0049	0.0011	0.0002	0.0001	0.0000	0
1.8	1.3844	0.4817	0.1715	0.0615	0.0224	0.0083	0.0031	0.0001	0
1.9	2.9825	1.5917	0.9340	0.5665	0.3480	0.2148	0.1328	0.0198	0